CHALMERS

Use of Corrugated Shell Plating in Semi-submersible Offshore Platforms

Study on exploring strength, weight and manufacturing implications of replacing the stiffened shell plating with corrugated panels

Master of Science Thesis

HÜSEYİN SAĞLAM
MD. ASADUZZAMAN SARDER

Department of Shipping and Marine Technology
Division of Ship Design
CHALMERS UNIVERSITY OF TECHNOLOGY
Göteborg, Sweden, 2010
Report No. X-10/251

A THESIS FOR THE DEGREE OF MASTER OF SCIENCE

Use of corrugated shell plating in semi-submersible offshore platforms

HÜSEYİN SAĞLAM

MD. ASADUZZAMAN SARDER

Use of corrugated shell plating in semi-submersible offshore platforms

HÜSEYİN SAĞLAM
MD. ASADUZZAMAN SARDER

Department of Shipping and Marine Technology
Chalmers University of Technology
SE-412 96 Göteborg
Sweden
Telephone +46 (0)31-772 1000

Use of corrugated shell plating in semi-submersible offshore platforms

HÜSEYİN SAĞLAM

MD. ASADUZZAMAN SARDER

Department of Shipping and Marine Technology
Chalmers University of Technology

Abstract

The deck load capacity of new offshore platforms is increasing as these marine structures continue to increase in size. As a consequence, the structural weight has become a concern. The current investigation contributes to a solution of a more weight-effective structural design of shell-plated marine structures.

The structural weight of a shell-plated structure can be reduced in various ways. In the current investigation, an alternative design is presented by means of a corrugated structure. By the introduction of corrugated panels, a structure may be constructed lighter and cheaper compared to traditional structures with stiffened panels. The welding work during manufacturing can also be reduced substantially. Even though the idea of using corrugated shell plating has been practiced in various applications for a long time, such as in corrugated bulkhead and deck plating, it is yet unexplored in shell structures. Thus, the aim with this study is to compare corrugated shell plating with conventional stiffened panels with respect to strength, weight and cost.

A methodology is presented where various solutions are analyzed and compared with regard to strength characteristics, weight and cost. Here, strength characteristics include ultimate tensile strength, buckling stability and fatigue life calculations. Detailed numerical analyses are presented using a realistic and reasonable area of a panel structure of an offshore platform. The structure analyses are carried out using linear finite element analyses. A number of design criteria have been evaluated and verified by comparing predictions obtained in an extensive parametric study of basic structural strength following classification rules.

Two alternative designs with corrugated shell plating are proposed with respect to corrugation symmetry. The first one had unequal flanges and the same thickness as that of the reference stiffened model. The second had equal flange lengths. The weight reduction values achieved using these designs were 38 percent and 59 percent in shell plating, respectively, compared with a reference model for traditional stiffened shell plating. The study concluded with a reduction in production costs by 35 percent and 49 percent, respectively. The investigation clearly demonstrates that corrugated panels are often favourable for lightweight design and manufacturing robustness of marine structures.

Keywords: corrugated panel, lightweight design, fatigue, buckling, ultimate limit state, cost, finite element analysis, parametric study, optimization.

Acknowledgements

Contents

Notations and abbreviations

Symbols

B	Breadth of the panel, m
L	Length of the panel, m
a	Width of the upper flange, mm
b	Width of the lower flange, mm
c	Width of the web plating, mm
d	Height of the web plating, mm
s	Width of the unit corrugation, mm
t	Thickness, mm
Φ	Corrugation angle, degree
SM	Section modulus, mm^4
N	Number of corrugations
ρ_s	Density of ABS steel, kg/m^3
ρ_w	Density of sea water, kg/m^3
h	Depth of top plating, mm
E	Modulus of elasticity, N/m^2
A	Total area of unit corrugation, mm^2
A_{sx}	Area of web plating of unit corrugation, mm^2
σ_o	Specified minimum yield point of plate, MPa
α	Aspect ratio of the panel
h	Depth of top plating, mm
W_{corr}	Weight of the corrugated upper shell plating of the section
W_{stiff}	Weight of the stiffened upper shell plating of the section
P_r	Proportional linear elastic limit of the structure
ν	Poisson's ratio
m	Length of short plate edge (b or c), mm
α_L	Aspect ratio for local buckling
σ_{xmin}	Minimum compressive stress in the longitudinal direction, MPa
σ_{xmax}	Maximum compressive stress in the longitudinal direction, MPa
σ_{ymin}	Minimum compressive stress in the transverse direction, MPa
σ_{ymax}	Maximum compressive stress in the transverse direction, MPa
κ	Ratio of edge stresses
C_1	Factor 1 for x-direction (for local plate of corrugated panels)
C_2	Factor 2 for y-direction (for local plate of corrugated panels)
k_s	Buckling coefficient for the x-direction
k_{s1}	Buckling coefficient for the y-direction
k_{s2}	Buckling coefficient for the y-direction (for κ>1/3)
k_S	Boundary dependent constant for edge shear
σ_{Ex}	Elastic buckling stress (x), MPa
σ_{Ey}	Elastic buckling stress (y), MPa
T_e	Elastic shear buckling stress, MPa
σ_{Cx}	Critical buckling stress (x), MPa
σ_{Cy}	Critical buckling stress (y), MPa
T_c	Critical buckling stress for edge shear, MPa
τ	In-plane shear stress, MPa
Ψ	Adjustment factor
η	Maximum allowable strength utilization factor (severe storm)

k_c	Coefficient
q_u	Lateral pressure at the first end of the corrugation (top plate), kN
q_l	Lateral pressure at the second end of the corrugation (top plate), kN
M_b	Maximum bending moment induced by lateral pressure, kNm
C_m	Bending moment factor for a simply supported panel, kNm
$\sigma_{E(B)}$	Elastic buckling stress of unit corrugation, MPa
σ_{cb}	Critical bending buckling stress, MPa
$\sigma_{E(C)}$	Elastic buckling stress, MPa
σ_{Ca}	Critical buckling stress, MPa
σ_b	Maximum bending stress along the length due to lateral pressure, MPa
σ_a	Maximum compressive stress in the corrugation direction, MPa
D_x	Stiffness factor in the corrugation direction
D_y	Stiffness factor in the transverse direction
τ_o	Shear strength of the plate, MPa
Φ_x	Angle value for corrugation direction, degree
Φ_y	Angle value for the transverse direction, degree
k_x	Factor for the corrugation direction
k_y	Factor for the transverse direction
σ_{Ex}	Elastic buckling stress in the corrugation direction, MPa
σ_{Ey}	Elastic buckling stress in the transverse direction, MPa
τ_E	Elastic shear buckling stress, MPa
σ_{Gx}	Global critical buckling stress for uniaxial compression in the corrugation direction
σ_{Gy}	Global critical buckling stress for uniaxial compression in the transverse direction
τ_G	Global critical buckling stress for shear stress, MPa
σ_x	Calculated average compressive stress in the corrugation direction, MPa
σ_y	Calculated average compressive stress in the transverse direction, MPa
β	Slenderness ratio
Ψ	Coefficient to reflect interaction between longitudinal and transverse stresses
σ_{Cx}	Critical buckling stress (x-direction), MPa
σ_{Cy}	Critical buckling stress (y-direction), MPa
τ_c	Critical buckling stress (shear), MPa
σ_{Ux}	Ultimate strength with respect to uniaxial stress in the long. direction, MPa
σ_{Uy}	Ultimate strength with respect to uniaxial stress in the transverse direction, MPa
τ_U	Ultimate strength with respect to edge shear, MPa
u	Lateral pressure at the first end of the corrugation (top plate), kN
σ_e	Equivalent von Mises stress, MPa
N_R	Number of cycles in a referenced period of time
S_R	Value which the fatigue stress range exceeds on average once every N_R cycles.
S'_R	Value which the fatigue stress range exceeds on average once every N'_R cycles.
Γ	Incomplete gamma functions [25]
S	A random variable denoting stress range
γ	Weibull shape parameter
δ	Weibull scale parameter

Abbreviations

ABS   American Bureau of Shipping
DNV   Det Norske Veritas
FLS   Fatigue Limit State
FM   Fracture Mechanics
LR   Load Redistribution
SF   Safety Factor
SLS   Serviceability Limit State
ULS   Ultimate Limit State
US   Ultimate Strength

x

1. Introduction

1.1. Background and motivation

Being a consultancy company, GVA Consultants (GVA-C) specializes in marine and offshore design related to mobile offshore units for the oil and gas industry. Starting from the disbanding GVA shipyard's technical department in the 90's, it has grown considerably with remarkable track record of platforms like Thunder Horse, Atlantis, etc. During the last decades, GVA-C has delivered quite a few benchmark offshore production and drilling platforms to the offshore world, for example, Fig. 1. GVA-C has been innovative on good concepts for modeling and analyzing flat stiffened shell plates.
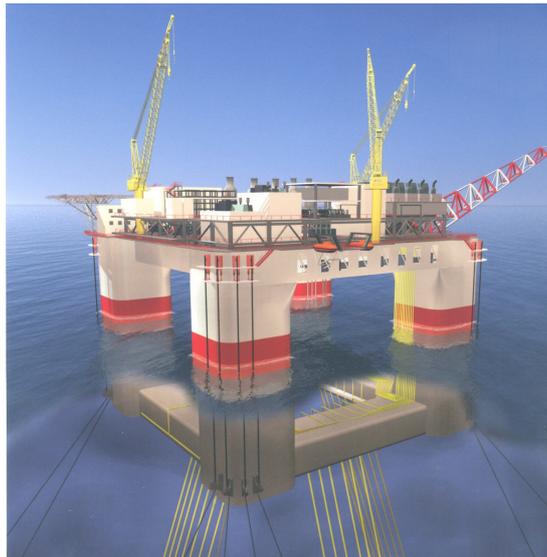
Fig. 1. GVA-C designed production unit used as a reference vessel in this study.

The main function of a semi-submersible production unit is to act as a production facility with stability and sustainability against harsh weather and wave impacts. Therefore, the shell structure has to be strong enough to serve the purpose.

Corrugated panels have been used for weight-saving, ease of construction and lower maintenance costs for bulkhead design in the marine industry. The idea of implementing corrugation on shell structures is now extracted from that concept and proposed for further developing and validating the conceptual merit.

Design and construction of offshore structures demand a set of tasks for the engineering profession. Over and above the usual conditions and situations met by land-based structures, offshore structures have the added complication of being placed in an ocean environment where hydrodynamic interaction effects and dynamic response become major considerations in their design. In addition, the range of possible design alterations such as hull shape, shell type and facility implementation on board are quite broad. Therefore, the new and innovative concept of implementing a corrugated shell structure demands high engineering skills in terms of structural strength and weight savings with respect to ease in the construction process.

So far, several studies have been carried out regarding corrugated panels; one of them is M. K. Rahman's panel form optimization [10], where two different types of stiffened panels are compared with a corrugated panel with respect to strength and production cost. At some level,

a significant amount of works on corrugated bulkheads can be found; one of them is ultimate strength of open corrugated bulkheads by J. Klippens [3], where three different types of ships were modeled and compared with corrugated bulkheads. It was also worth studying the work of J.B. Caldwell, 'The strength of corrugated plating for ships' bulkheads' [4] and the work of J.K. Paik, 'Theoretical and experimental study on ultimate strength of corrugated bulkheads' [5] for obtaining a theoretical background of strength validation of corrugated shell plates of offshore structure.

For a production unit, the resistance during transport from yard to site is not significant. This has been the background to the idea of designing the pontoons.

1.2. Objectives and tasks

The main objectives and corresponding tasks of this investigation are as follows:

- To design part of a pontoon with corrugated shell plating according to ABS Rules.
- To carry out a parametric study with regard to buckling, ultimate strength and weight.
- To propose an alternative design with corrugated shell plating with different geometrical parameters from that of the first corrugated design.
- To evaluate the structural responses of the new design.
- To modify the existing stiffened model to find the potential for lightening.
- To propose a new design for different operating depths of the structure.
- A simplified fatigue analysis will be carried out to see the fatigue range compatibility.
- To find manufacturing and cost advantages/disadvantages of the new design.
- The above steps are to be repeated due to the various modifications of the geometry.

1.3. Methods adopted for investigation

The flow chart in Fig. 3 presents the general procedure used in the current study. The first step is to establish the numerical reference FE-model. Figure 2 shows a pictorial procedure.
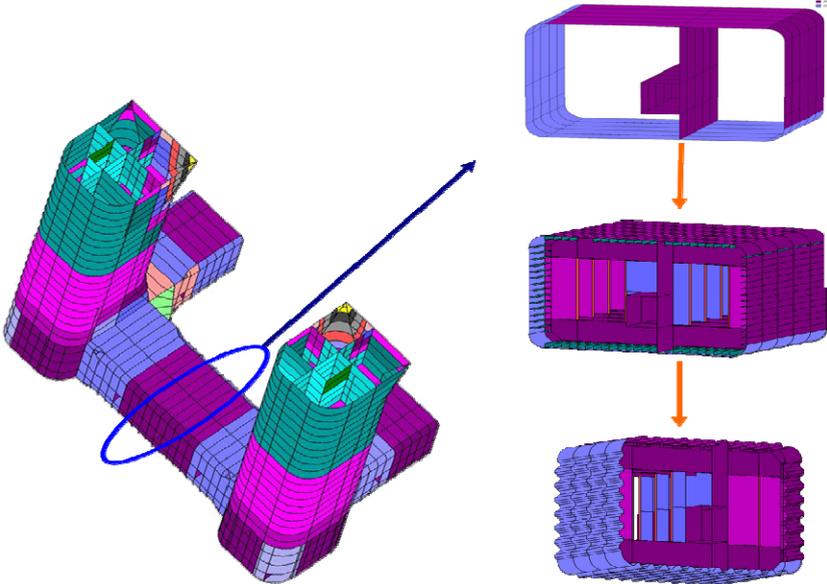

Fig. 2. Approach of general procedure.

2

A representative part of the pontoon was modeled that was big enough to sufficiently mimic the strength characteristics of the pontoon of the production platform. This part was made according to drawings using finite shell elements in the FE-program, PreFIX [6]. The analysis is made using a DNV SESAM suite of software [6]. A section far off from the pontoon ends was chosen and was coupled to the global model. This part should bear the general structural characteristics of the pontoon so that it can be accepted as a representative model for the whole pontoon.

An extensive parametric study has been performed for a part of the top plating of the pontoon, see Fig. 9. Different corrugation parameters have been systematically varied to optimize for weight while satisfying ABS rules for buckling and ultimate strength of corrugated panels. In the parametric study, different failure modes for a corrugated panel are identified and taken into account. Stress evaluation of the corrugated FE-model was done and the stress distributions were extracted and used as input values in the parametric study in order to optimize the structure with regard to strength and weight characteristics.

The input values were basically the unknown parameters that are required for solving the analytical calculations. An iterative process followed until the analytical results of the final proposed corrugated type were validated with FEA. Therefore, the analytical calculations and FEA were dependent on each other.

As a last step, a simplified fatigue analysis was carried out for the two designs.

Variation of the depth was used to investigate the influence on weight reduction and failure modes for both the corrugated and the stiffened structure. This study was carried out for the depths of 0, 10, 20 and 30 meters.

At last, a manufacturing and a cost analysis were carried out with the help of simplified section models. The influence of parameter changes were calculated in terms of production cost and were compared.

1.4. Limitations and assumptions

Throughout the study the following simplifications were made:

- A linear elastic FE analysis was employed to all numerical analysis.
- Optimization is carried out for only a part of the pontoon extracted from the global model.
- The sub-model geometry is simplified by excluding members (e.g. stiffeners, brackets, small holes, etc.) which are far from areas of interest for the sake of computational efficiency.
- The corrosion margin was excluded in the calculations for both types of models.
- For fatigue assessment, only a simplified fatigue analysis [22] is carried out.
- In the design, the static tank pressure head to the top of the pipe and the dynamic tank pressure due to flow through pipe is not taken into account. When over-filled, the pressure here might impose a significant pressure on the model.
- The FE-analysis did not incorporate the imperfections due to the welding or fabrication process.
- It was assumed that the final proposed corrugation geometry would not cause significant manufacturing difficulties; although these concerns are outside the scope of this theoretical study.

- Shell elements were considered throughout the FE procedure.
- Only severe storm (100-year hurricane) and fatigue (100-year winter storm) loading conditions have been used for the analysis assuming that this will bear the most critical stresses. However, for a normal operations load condition, a lower value of strength factor (0.6) is suggested than that of severe storm which is 0.8. Thus, with a higher strength factor, normal operations can give stresses for a critical load case, which might not compensate the difference in the strength factors stated above.
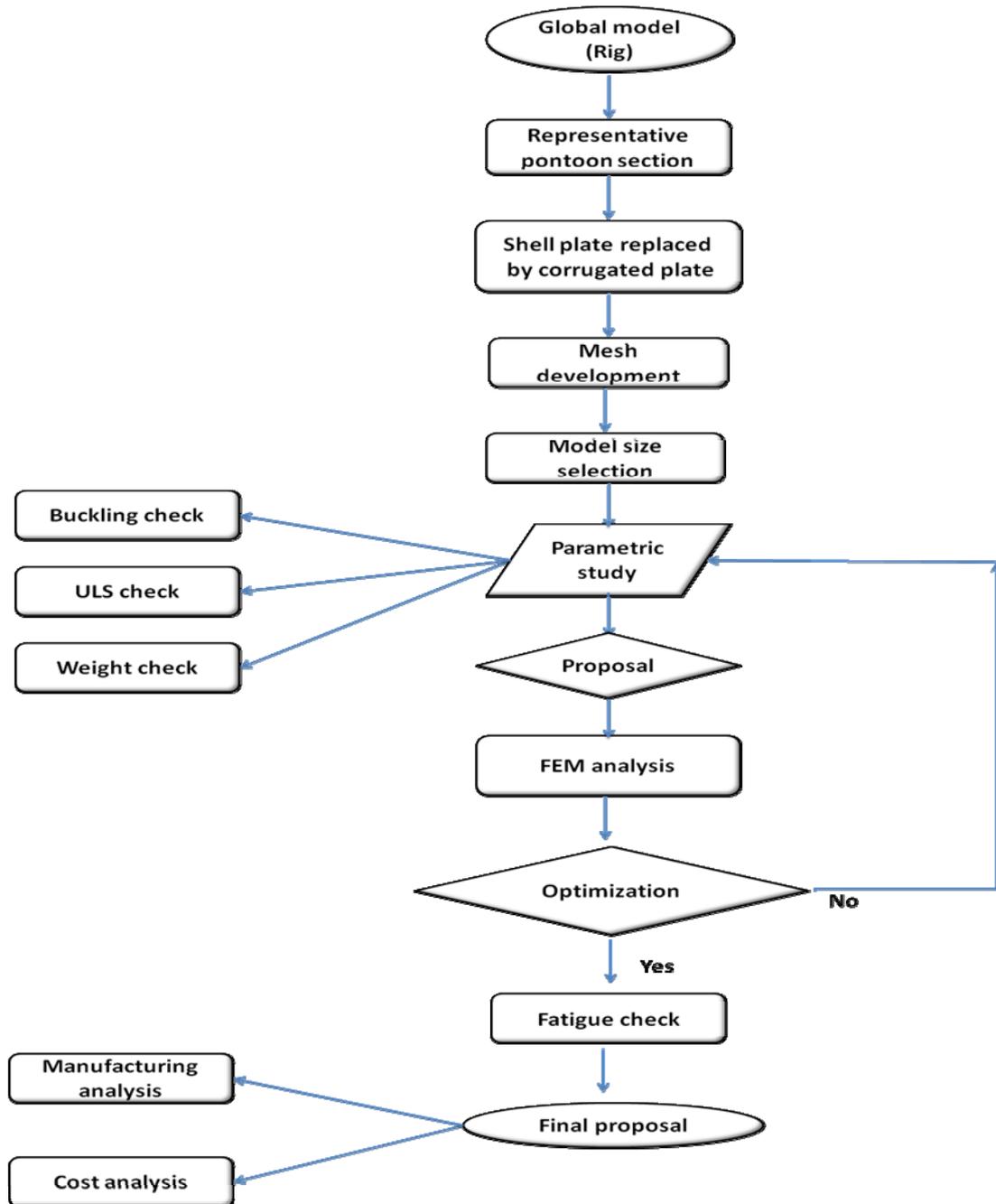
Fig. 3. Flow chart of general procedure.

2. Description of the reference pontoon structure

In the present work, a pontoon of a semi submersible production unit from GVA-C was used as reference, see Fig. 4. The pontoon shells are designed with stiffened flat steel plates. Some main particulars of the unit are given below:

- Type: semi-submersible (production unit)
- Length overall: 146 m
- Width overall: 137 m
- Length of pontoons: 105 m
- Draught: 41.5 m
- Topside load: 33,000 metric tonnes
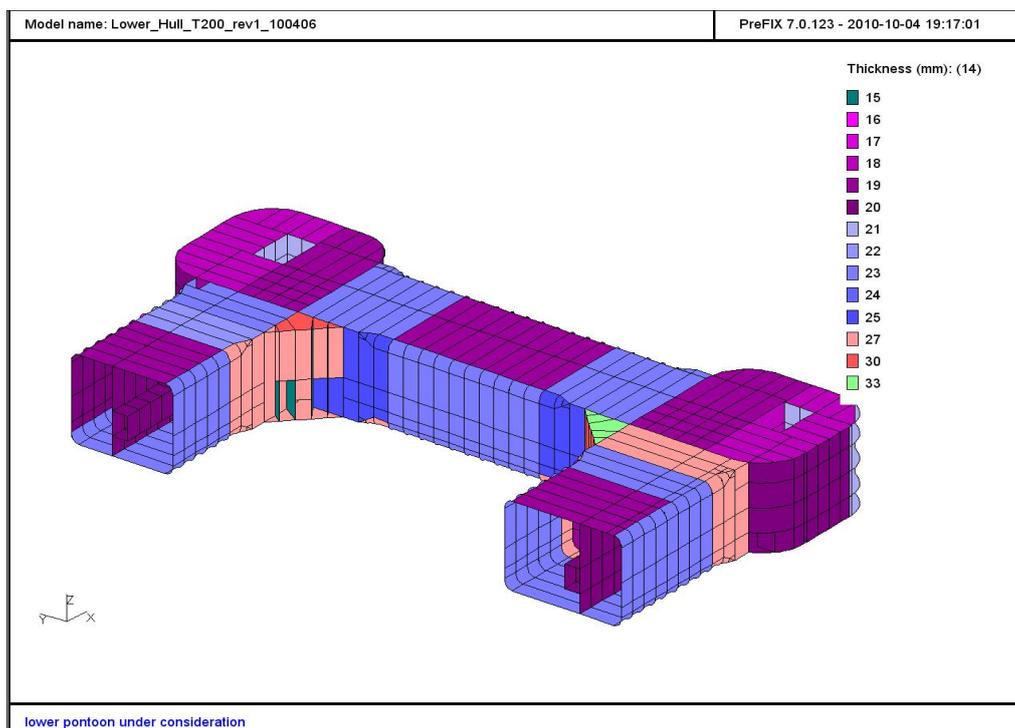
Fig. 4. Complete global pontoon considered as reference.

The global FE model supplied by GVA and part of the pontoon with five sections, see Fig. 2, was employed for the FE modeling and analysis procedure. A pontoon part with five sections as seen in Fig. 2 (top right) was extracted. This section only consisted of members contributing to the global stiffness of the structure. This section did not incorporate any stiffeners, which were later added to the structure (Fig. 2, top right). Numerical data for the model:

- Length: 12.80 m
- Width: 17.28 m
- Height: 11.52 m
- Depth: 29.98 m
- Stiffener spacing: 640 mm
- Stiffeners (bulb type): (430×15 + 55×68.5) mm
- Shell plate thickness: 19-23 mm

The design of this rig is being carried out by GVA-C. The project has focused on this structure. In the parallel project (with stiffened shell plating), GVA-C uses the initial reference model in their design which is established thoroughly with regard to weight and strength, but, rather, it was satisfying enough to serve its purpose. Therefore, the potential of the initial reference model for lightening is not known. Thereby, the study included the investigation of weight reduction potential of the reference stiffened model, see Fig. 5, to obtain a lightened structure which is later compared to the corrugated model given in Fig. 17. The results and method followed are given in Chapter 8.
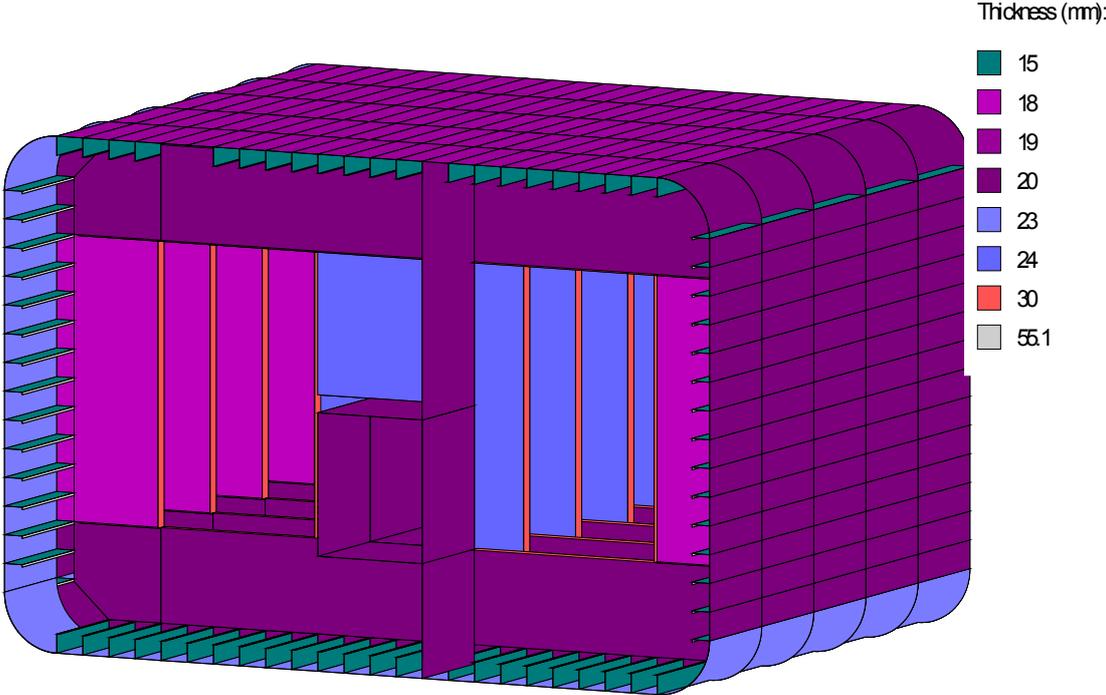
Fig. 5. Reference stiffened model.

The main target of the study was to investigate the potential of using corrugated shell plating instead of conventional stiffened plating in the outer shell surface of the pontoon part of the semi-submersible. In the following chapters, the method and work flow to search for this potential has been explained in detail.

The following material properties from Table 1 were used for the plating of all FE models.

Table 1. Material properties.

Component	Value	Unit
Young's modulus	2.06E+11	N/m^2
Density of steel	7850	kg/m^3
Poisson's ratio	0.3	-
Thermal expansion coefficient	1.20E-05	-
Yield stress	355	MPa
Shear stress	204.96	MPa

3. Strength assessment of shell structure

3.1. Theoretical background for strength analysis

Strength analysis is based on elastic theory. Ultimate strength capacity of the panel was measured to assess the strength characteristics and used for comparison as a measure of merit in the lightweight design optimization. Buckling and yielding are the dominating phenomenon for attaining the ultimate strength limit when the compressive stresses are significantly high. For this study, it was acknowledged that both the yielding and buckling will govern the design of the part of the pontoon in question. Criteria and methods to quantify and measure the parameters related to buckling and yielding were proposed by ABS [7], DNV [23] and GVA-C [18]. Table 2 shows the failure scenarios.

Table 2. Schematic arrangement of five explicit failure scenarios.

Collapse modes	Description
	Overall collapse of corrugations as a unit where the corrugations buckle together with the plating as a unit.
	Panel failure by yielding along the edge of corrugation and lower flange intersection at the panel edges under biaxial compression. As a secondary effect panel collapse occurs.
	Collapse of corrugations as a beam under axial compression and lateral load. Ultimate strength is reached due to yielding of the corrugation at mid-span. Stresses at the ends are higher than in the mid-span so occurrence of yielding in mid-span indicates beam collapse of unit corrugation.
	Local buckling of the corrugation web or flange where ultimate strength is reached when the web/flange buckles subjected to local compressive stress.
	Gross yielding might take place when the panel is subjected to tensile axial tensile load predominantly and panel cross section yields before the global or local buckling of panel take place.
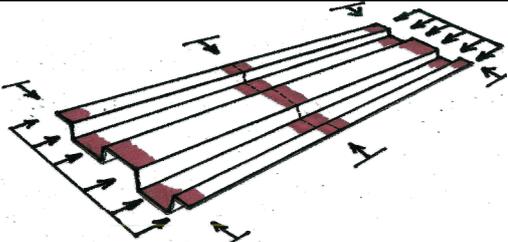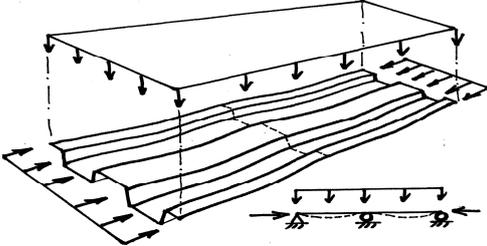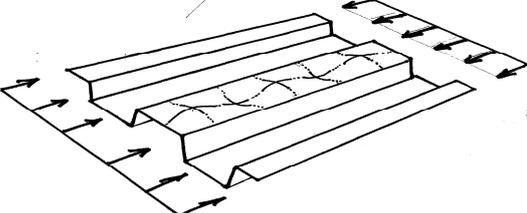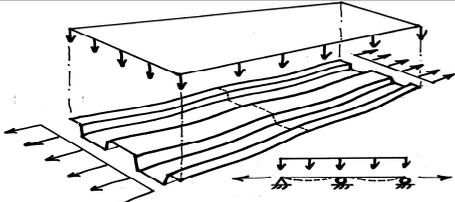
In addition to the above mentioned scenarios, von Mises equivalent design stress shall not exceed the design resistance.

The panel can buckle due to compression load, shear load or lateral pressure. The assessment in this study includes uniaxial compression combined with shear load and lateral pressure. The in-plane rigidity is reduced by lateral deflection caused by lateral load or buckling. This lateral deflection accounts for bending stresses as well as redistribution of the in-plane stresses.

Shell plating is investigated for buckling. Buckling of plates is normally not allowed. The buckling stresses are calculated during the parametric study for a number of load conditions (static, dynamic), corrugation profiles, slenderness and aspect ratio of corrugated panels.

3.2. The limit state

The limit state is the design limit after which the structure does not satisfy the design rules. Below, the limit states are shown:

- ULS: Ultimate limit state
- FLS: Fatigue limit state
- ALS: Accidental limit state
- SLS: Serviceability limit state

In this study, ULS and FLS are used. The limit states impose guidelines on how strength factors for loads and material parameters are to be used. The study employed a 'Severe Storm (ULS)' loading condition. This condition defines the design environmental condition as a 100-year extreme storm condition wave spectrum [7]. The strength factors are presented in Table 3.

Table 3. Load cases and factors.

Load condition	Load type	Number of load cases	Range	Factor (buckling)	Factor (yielding)
Severe storm	Static	21	1-21	0.80 ψ	0.90
Severe storm	Dynamic	35	22-56	0.80 ψ	0.90

FE-analysis of the structure was scanned using the load cases defined for the severe storm load condition. Instead of a safety factor, a maximum strength utilization factor (η) was employed, which is the inverse of the safety factor. The value of this factor depends on:

- the loading condition,
- type of the structural component, and
- failure consequence.

This factor is used along with the loading condition and applied to the predicted calculated strength of the structure in the parametric study. ψ is an adjustment factor which depends on the loading types (tension, compression) and structural members.

3.3. Design loads on the pontoon level

It is of importance to be conscious of the loads in order to assess the quality of the analysis results. Two types of loads acted on the pontoons; combined global loads, which are transferred via node translations and node displacements, and lateral loads. The combined global loads were transferred from a parallel project global model. The global FE-analysis result file for the complete structure was readily supplied to us with the different load combinations already defined for the pontoon level. Lateral loads were applied manually on shell surfaces.

The global loads are classified into two groups in the MODU Rules (Rules for building and classifying mobile offshore drilling units) [8];

1) Static Loads: These are defined as still-water loads and will cause a global bending moment and shear force in the hull girder. Besides, the external sea pressure and internal tank pressure will result in the local response of the plates, stiffeners and girders.

2) Environmental (Dynamic) Loads: These loads are caused by winds, currents, ice and waves, green water, etc. The equilibrium in analysis is attained when the sum of the dynamic forces is zero.

The load components for static and environmental loads are combined. In this combination process, global bending moments, shear and axial forces are superimposed and maximum values are obtained which are to be used in the buckling/yield check of the study further on. The load combinations are combined in such a way as to create the most severe section forces in critical sections.

In order to minimize the amount of stress plots and ease result presentation, the maximum stress in each element, derived from the different load cases, is scanned for ultimate, normal and fatigue strength evaluation. GVA-C employs this methodology, since this is a time-effective and conservative approach to design a structure. For the ultimate and normal strength assessment von Mises static and dynamic stresses are combined and scanned in an extreme storm condition. For the fatigue strength assessment, maximum dynamic principle stresses are scanned for a 30-year fatigue life.

3.4. Overview of the class rules

The design of the semi-submersibles should satisfy the requirements set by the classification society. This study has followed the rules and guidelines of the American Bureau of Shipping (ABS). The ABS has a guide for buckling and ultimate strength assessment for offshore structures that also includes a subsection on criteria for the buckling and ultimate strength for corrugated panels.

A general formulation is prepared to check the strength capacity of the corrugated panels against different criteria proposed by the ABS. These criteria are listed in the previous section in this chapter. An Excel spreadsheet for corrugated panel is prepared in a similar manner to a GVA-C in-house developed sheet (PULS) for stiffened panels. The calculation procedure of the criteria is given in Appendix H.

3.4.1. Local buckling assessment

In this buckling mode, different plate strips of the corrugation profile buckle out of plane. The buckling strength of the flange and web plate subjected to in plane and lateral pressure loads is assessed through the following limit state according to the ABS [7]:

$$\left(\frac{\sigma_{xmax}}{\eta\sigma_{Cx}}\right)^2 + \left(\frac{\sigma_{ymax}}{\eta\sigma_{Cy}}\right)^2 + \left(\frac{\tau}{\eta\tau_C}\right)^2 \leq 1 \tag{1}$$

This formula takes into account the combined effect of in-plane loads in the longitudinal and transverse directions and shear. Figure 6 typically sketches a 3D view of the three types of stress components that create this combined effect.
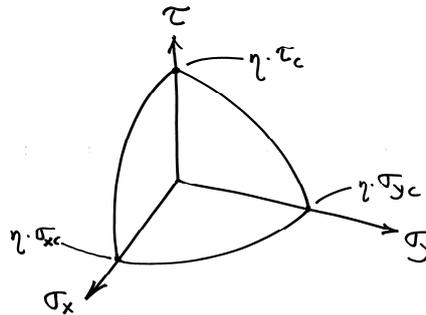
Fig. 6. A 3D illustration of the direction of stress components that form a limit state equation.

Table H1 represents the way that the local buckling capacity of the corrugated model was calculated and the parameters considered. The capacity is given in the final line of the Table H1, which is 0.479, implying that 48 percent of the local buckling capacity of the plate is used. In other words, the margin of error of the structure is 52 percent.

Another parameter in the ULS-assessment is the proportional linear elastic limit of the structure, here called P_r which is used as a correction factor to the critical buckling stress (bifurcation) levels above the yield point.

The ABS defines a compactness concept, where if the section of the corrugated panel is compact, the local buckling of flange and web plates is most likely not the critical failure mode. A cross section is compact if the web and flange plates satisfy the following requirement [7]:

$$\frac{a}{t}, \frac{b}{t}, \frac{c}{t} \leq 1.5\sqrt{\frac{E}{\sigma_0}} \tag{2}$$

Table 4. Compactness check for initial corrugation.

Ratio	Value	Assessment
a/t	16.84	not compact
b/t	16.84	not compact
c/t	28.21	not compact
Max. required value	0.04	

As seen from the Table 4, the cross section of the corrugated panel is far from being compact. One of the conclusions during the parametric study was that this kind of configuration is not likely to appear in the corrugated structure in question. Thus, the local buckling might be more relevant than beam-column or global buckling. This structure is expected to fall into the transition range, where the inelastic behavior and structure strength is the combination of elastic and plastic strength. In this study, the members fall into the Euler (elastic strength) and non-compact (inelastic strength) regions.

Critical stresses are calculated for static loading conditions employing the linear buckling analysis. The initial elastic buckling of the flat plates are considered. It can also be stated that for local buckling modes, the corrugated panel will have a load-carrying capacity after buckling, since all the component plates behave similarly to plate panels.

3.4.2. Beam-column buckling assessment

This limit state implies the buckling of any unit corrugation of the corrugated panel. Unit corrugation was treated as a beam column and the following state limit is to be satisfied [7];

$$\frac{\sigma_a}{\eta \sigma_{Ca}} + \frac{\sigma_a}{\eta \sigma_{CB}\left[1 - \sigma_a / \left(\eta \sigma_{E(C)}\right)\right]} \leq 1 \tag{3}$$

This equation incorporates the capacity of the unit corrugation as a beam to buckling and the resistance of the beam to the bending stress due to lateral load. The application of this general formulation on our corrugated structure is presented in Appendix H2.

This buckling mode is expected to be critical because of the significant bending stresses due to lateral load (denoted as σ_b) on the shell plating of the pontoon. The beam is pre-deformed due to lateral load and thus bifurcation will not take place. For this case, a snap through to the Euler IV mode of buckling is expected to occur since the lateral loads are high. The bending stress for this geometry contributes to around 60 percent of the beam-column buckling capacity. The bending stress due to lateral load was calculated for the panel with fixed edges. The beam has a symmetry regarding the structure and lateral loads at the transverse web frame passages. This passage was treated as fixed (no rotation); otherwise the Euler II mode would be too conservative. The Euler II mode would imply that every second beam-column along the longitudinal direction of the structure would buckle inwards and outwards as would be the case where the lateral load is small. Thus, the Euler IV mode was assumed as being more accurate. The elastic bending buckling stress was adopted according to Caldwell [4] who has suggested a formula for corrugated panels.

3.4.3. Global buckling assessment

In this buckling mode, the whole panel is expected to buckle out of its own plane. The overall buckling strength of the entire corrugated panels disregarding lateral load is to satisfy the following equation with respect to the biaxial compression and edge shear [7];

$$\left(\frac{\sigma_x}{\eta \sigma_{Gx}}\right)^2 + \left(\frac{\sigma_y}{\eta \sigma_{Gy}}\right)^2 + \left(\frac{\tau}{\eta \tau_G}\right)^2 \leq 1 \tag{4}$$

This buckling mode has not been critical, since separate plate strips do not have a small width/thickness ratio. Besides, the distance between the transverse web frames supporting the panel is very short compared to the width of the panel. The aspect ratio of the panel is around

11

0.5, and thus the global buckling mode is out of the question as a design failure for the possible corrugated shell plating designs as long as the length remains the same. By increasing the length four times it was found that the global buckling capacity increases from 16 percent to 74 percent; see Appendix H3.

3.4.4. Ultimate strength assessment

The ABS suggests that offshore practice demonstrates that only an ultimate strength check is required for plate panels [1]. Plate buckling is allowed as long as the ultimate strength criteria are satisfied.

The ultimate strength for a plate between stiffeners subjected to combine in-plane stresses has to satisfy this equation [7];

$$\left(\frac{\sigma_{xmax}}{\eta\sigma_{Ux}}\right)^2 - \varphi\left(\frac{\sigma_{xmax}}{\eta\sigma_{Ux}}\right)\left(\frac{\sigma_{ymax}}{\eta\sigma_{Uy}}\right) + \left(\frac{\sigma_{ymax}}{\eta\sigma_{Uy}}\right)^2 + \left(\frac{\tau}{\eta\tau_U}\right)^2 \leq 1 \tag{5}$$

This is a basic equation, incorporating ultimate strength contributions in each direction. Slenderness ratio and length of the short plate edge are the critical parameters for ultimate strength of the plate areas. For the plate areas, as long as the ultimate strength of the plates are assessed, buckling is acceptable; see Appendix I.

It is desired for the plates to buckle before they reach their ultimate strength level. Considering only the longitudinal direction, the maximum compressive stress is required to be less than the ultimate stress in the longitudinal direction multiplied by a strength utilization factor;

$$\sigma_{xmax} \leq \eta\sigma_{Ux} \tag{6}$$

And from the first criteria for local buckling considering only one direction;

$$\sigma_{xmax} \leq \eta\sigma_{Cx} \tag{7}$$

This ensures the prevention of buckling by requiring the reduced bifurcation stress (reduced by strength utilization factor, η) to be higher than the maximum compressive stress in the longitudinal direction. Criteria for the ultimate strength require the ultimate stress in any direction to be higher than the bifurcation stress which takes account of the slenderness ratio;

$$\sigma_{Cx} \leq \sigma_{Ux} = C_x\sigma_o \text{ where } C_x \text{ is the slenderness ratio} \tag{8}$$

$$\sigma_{xmax} \leq \eta \cdot C_x\sigma_o \tag{9}$$

As a conclusion, the ABS formulation requires the two cases to be compared. The reduced (by yield correction factor, Pr) critical buckling stress calculated depending on the ratio of edge stresses (κ) and the reduced ultimate stress calculated depending on the slenderness ratio (C_x) were required to be higher than the maximum compressive stress and were also compared with each other in order to pick the conservative value.

Another criterion is employed for the ultimate strength check of the structure. Yielding must be checked for the plates subjected to lateral loads and/or in-plane loads. The ultimate strength of the plate subjected to uniform lateral pressure combined with in-plane stresses has to satisfy the following criteria [7];

$$q_u \leq \eta 4.0 \sigma_o a (\frac{t}{s})^2 (1 + \frac{1}{\alpha^2}) \sqrt{1 - \left(\frac{\sigma_e}{\sigma_o}\right)^2} \tag{10}$$

This formula incorporates the lateral pressure and also the in-plane stresses as von Mises equivalent stress, σ_e. The spacing of the corrugation (s) and the length of the short plate edge (t) have a significant influence on this limit state; see Appendix I2.

3.4.5. Yielding strength assessment
The permissible stress is to be compared with the von Mises stress for yielding. The von Mises stress is to be below the allowed ULS limit. The effect of stress concentration is only considered in fatigue analysis.

For plated structures the von Mises equivalent design stress is defined as follows [7]:

$$\sigma_e = \sqrt{\sigma_{x\max}^2 - \sigma_{x\max}\sigma_{y\max} + \sigma_{y\max}^2 + 3\tau^2} \tag{11}$$

The von Mises criterion is checked for yield for the complete shell plating of the model. This criterion requires that the 90 percent of the von Mises equivalent stress value does not exceed the design stress for the structure. In our case, severe storm is used as a loading condition for ULS and thus the 90 percent of the yield stress is the design stress. Scanned von Mises stresses are evaluated.

3.5. Fatigue strength assessment

Load-induced fatigue stress ranges were considered in order to validate the final design that had already satisfied the other criteria for yielding and buckling. A simplified fatigue calculation based on the design wave approach described in the ABS [24] was performed.

The 33 environmental loads applied in the simplified fatigue calculation are described in the overall structural load analysis report prepared by the GVA-C overall fatigue design assessment sheet. The fatigue strength is characterized in terms of a maximum allowable stress range. The probability level corresponding to N_R is found as:

$$S_R' = \left[\frac{(\ln N_R)^{m/\gamma}}{FDF \cdot N_T \left[\Gamma\left(\frac{m}{\gamma} + 1, z\right) \Big/ A + \delta^{r-m} \Gamma_0\left(\frac{r}{\gamma} + 1, z\right) \Big/ C \right]} \right] \tag{12}$$

When the fatigue is assessed in terms of allowable stress range, the safety check expression is $S_R \leq S_R'$

The following assumptions were effective during the analyses:

1. The design is of a fail-safe type.
2. The evaluation criterion is based on mesh dependency.
3. The linear cumulative damage (Palmgren-Miner) rule applies, and that fatigue strength is defined by the S-N curves.
4. A safety factor (of $3 \times 30 = 90$ years) was implied according to GVA-C procedure [18].
5. The response from the 100-year winter storm was recalculated to a 30-year response period using a Weibull parameter defined in accordance with the ABS [24].

4. Adopted approach of an FEA of corrugated structure

The FE work was carried out according to GVA-C's work procedure and methods [18]. GVA Consultants use the DNV's SESAM linear FE-analysis software package for offshore industry [6]. General features and settings throughout the FE work were as described in this chapter. The FE analysis comprises four major steps;

1. Structural modeling
2. Calculation
3. Post-processing
4. Strength assessment according to the ABS (i.e. buckling, yield and fatigue checks) [7,22]

An FEA was employed for the selected part of the pontoon. Figure 7 depicts the FEA procedure used.
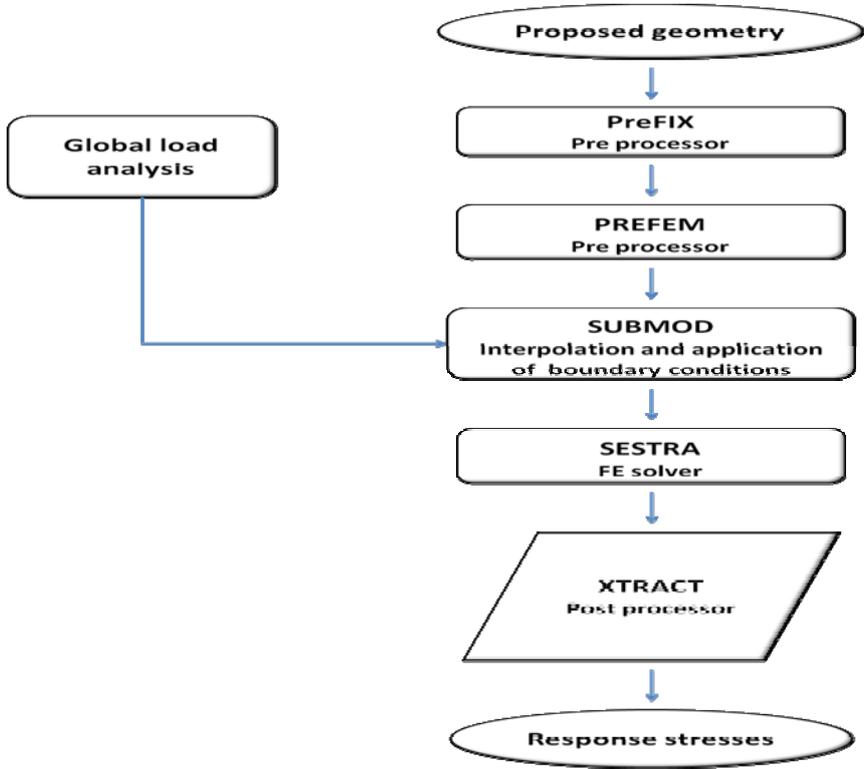
Fig. 7. GVA-C FEA procedure with a SESAM software suite.

The pontoon was modeled in Prefix as one super-element and geometries, scantlings, element types and boundary conditions were created in this module. Boundary conditions were assigned as prescribed displacements (denoted as D); see Fig. 8. Structural plating was modeled using 8-node quadratic shell elements, except for some triangular areas with 6-node elements. The element had six degrees of freedom at each node, i.e. three translations and three rotations.

The preliminary geometry were extracted directly from the global model and used as a basis. The hydrostatic pressure loads at a design draught of 30 meters were applied with a normal distribution to all the surfaces in order to match the load pattern in the global model. PREFEM is used as a pre-processor for meshing. SUBMOD was used for matching the sub-

model boundaries to the global model nodes. In this stage, attention was given to the tolerance value as it should be chosen in a way that it would include all the nodes to be coupled and also that irrelevant nodes were not captured. Node-to-node coupling was employed.
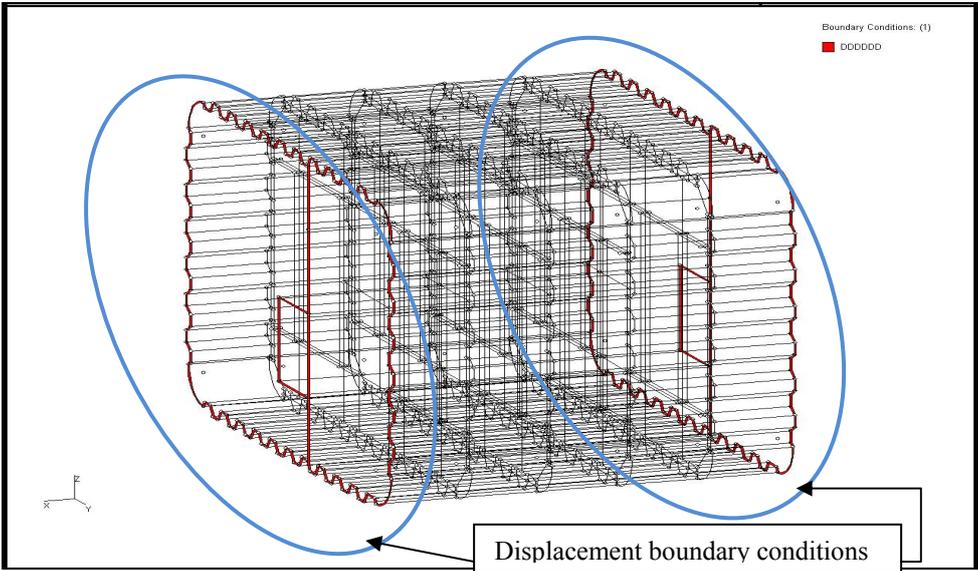
Fig. 8. Displacement boundary conditions applied to the edges of the model.

Once the model was meshed and the loads were transferred from the global model, the model was then analyzed. The stiffness analysis of the model was carried out using SESTRA.

As a last stage, post-processing was carried out. In this stage, the results were scanned and combined along with their maximum and minimum values. Xtract was used for post-processing results. The results from the FE analysis must be used with caution. Only results at a distance from the boundaries were used for evaluation. The mid section, two sections away from both boundaries, was chosen as the reference area to analyze the results; see Fig. 9.
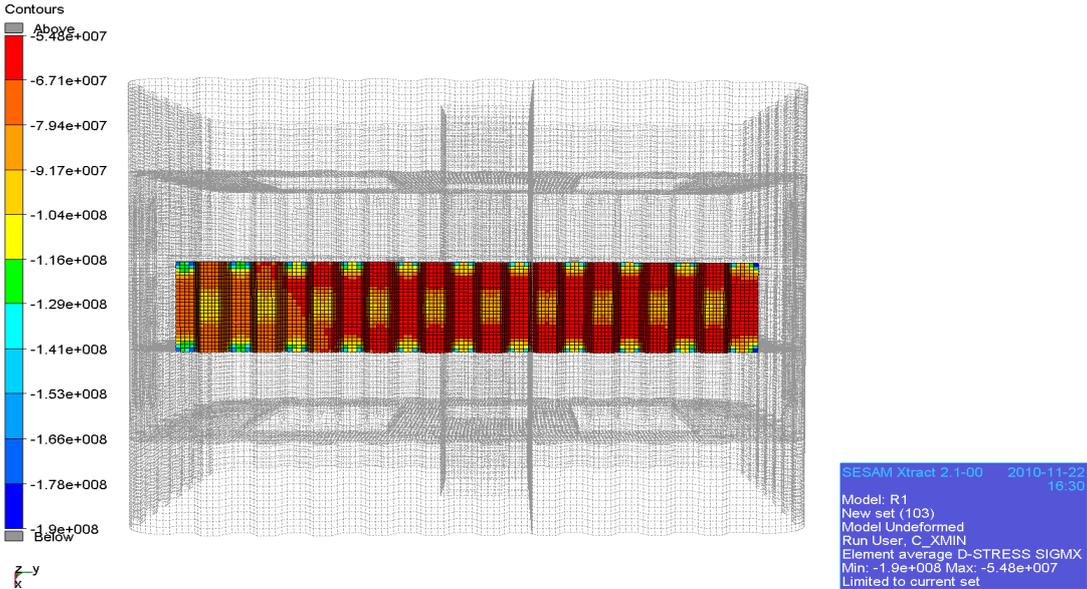
Fig. 9. The shell panel area used for extracting stress responses is indicated with colours. Five sections between frames of the pontoon are seen from above with a semi-transparent top plate.

5. Development of FE models of corrugated structure

5.1. Mesh density study

Mesh density is one of the prime conditions for the accuracy of the Finite Element Analysis. For computational efficiency, a mesh density study was carried out only for a part of the cross-section. Four different mesh densities were compared with respect to stresses and computation time.

Table 5. Stress responses for mesh density analysis.

Mesh size (mm)	CPU time (minutes)	No. of elements	No. of coupling nodes	σ_{xmin} (membrane stress) (MPa)	von Mises (MPa)
75	120	78704	2375	116	142
100	98	47483	1652	116	142
150	57	19727	1187	126	138
200	18	8942	756	144	133

The mesh density study showed that the coarse mesh (200 mm) was not so accurate compared to the others. The computation time was reduced significantly, see Table 5, but the difference between the stress values was high. Accuracy was defined as a major criterion, so a medium mesh density of 100 mm element size was adopted for the upper portion of the cross-section of the pontoon. However, for the lower portion of the cross-section, a 200 mm element size was adopted. As a conclusion, the model meshing consisted of two different element sizes (100 and 200 mm). This mesh configuration was validated through a comparison of various FEA on the part in Fig 10.

Figure 10 illustrates the relation between the mesh sizes and stress responses. A portion of two models with 100 mm and 75 mm mesh sizes are given in Appendix A.
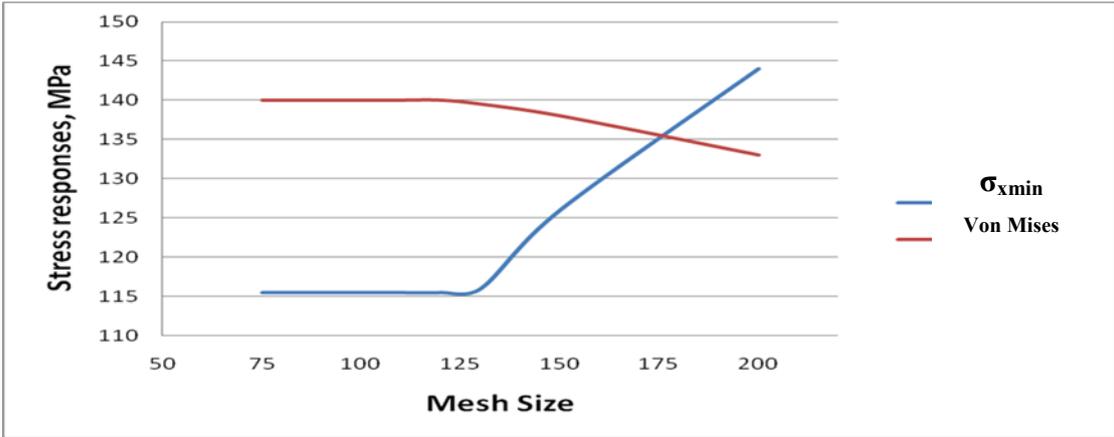
Fig. 10. Graph clarifying mesh convergence.

5.2. FE model size of the pontoon section

The reason for this analysis was to establish a model size on the basis of finding a section that is far enough from the boundaries that couples to the nodes of the global model. It was observed that five sections can encompass more stresses than three sections. The distance to the boundary conditions, i.e. the influence of the boundary conditions, was vital here. The analysis was performed with usual load conditions.

For model size; three and five sections were tested. Five sections with 100 mm element meant a considerable delay in CPU timing and high storage space. As is seen in Table 6, a model with five sections was chosen.

Table 6. Stress response from different model sizes.

Number of sections	Element size (mm)	σ_{xmin} (membrane) (MPa)	von Mises stress (MPa)	Number of elements	Time (hours)
3	100	-69	74	110441	6.87
5	100	-65	75	188320	7.88

Once the model size is set, enormous computing time was observed for this model. An innovative resizing of meshing was introduced. The outer 2 boundary sections' top portions were meshed with a 200 element size. In this way, the number of elements was reduced significantly, while the accuracy of the results was sustained. The top part of the three middle sections was used for buckling, and the ULS and fatigue effect was meshed with 100 mm. Table 7 and Appendix C illustrate the figures and motivation for this meshing configuration. Therefore, based on the time and characteristics mapping capability, five sections with 100 mm at the top and 200 mm at the remaining parts of the sections were chosen as a working mesh pattern.

Table 7. Updated mesh pattern.

Number of sections	Element size (mm)	σ_{xmin} (membrane) (MPa)	von Mises stress (MPa)	Number of elements	Time (hours)
3	100 top-200	-64.8	68	88055	6.17
5	100 top-200	-64.9	72	126661	7.26

6. Parametric study on corrugated panels

6.1. Detailed methodology

The study involved a basic parametric study on corrugation configurations of shell plating. The task was to carry out an in-depth study by varying predestined parameters between extreme values and to try to draw conclusions regarding design criteria for buckling and the ultimate strength of corrugated panels. The underlying reasons for employing a finite element analysis only at some necessary steps of the whole design process of the shell plating were:

1) FE modeling and analysis is a time-consuming process. The extent of the design modifications would be limited; since the model in question has around 80,000 elements with six degrees of freedom.
2) FE modeling and analysis is not enough for perceiving the basic idea of parametric influence because of the complexity of the problem. A parametric study was carried out to gain extensive knowledge on how strength is influenced by each of the parameters of the corrugations, boundary conditions, aspect ratio, loading in the x and y directions and different loading cases according to the ABS and DNV.

A general formulation has first been made where the strength characteristics of a sample design has been calculated. A conservative approach has been followed for all the proposed solutions throughout the parametric study and extraction of results from the FEA. The emphasis was put on being equally safe for all the design alternatives for comparability. Later, different parameters have varied one at a time, which was preceded by a variation of two coupled parameters (combined variation).

6.2. Limitations

It should be noted that the ultimate strength of structural members are sensitive to initial distortions. These were taken into account explicitly during neither parametric study nor modeling of the corrugated panel. However, residual stresses and initial deformations are already incorporated explicitly in the ABS formulations. Besides, for the buckling calculations of the unit corrugation as a beam, the influence of an effective width concept was not employed. The consequences of this are minor, as our panels are reasonably long compared to width.

6.3. Description of the four-corrugation panel

A typical corrugated section with its parameters is specified in Fig. 11. The last two variables were expressed in terms of some other variables.

- Width of corrugated panel, B
- Length of corrugated panel, L
- Thickness of the plating, t
- Width of unit corrugation, corrugation spacing, s
- Upper flange width, a
- Height of web plating, d
- Corrugation angle, Φ
- Width of lower flange, $b = b(a, s, c)$
- Width of web plating, $c = (\Phi, d)$
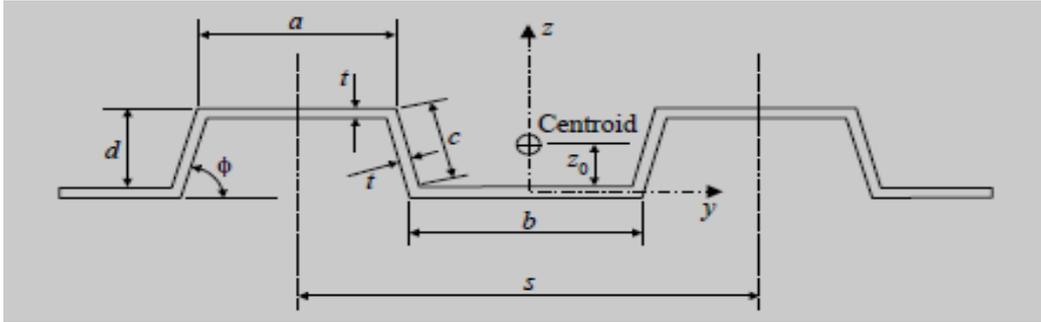
Fig. 11. Cross-sectional sketch of a corrugated panel [7].
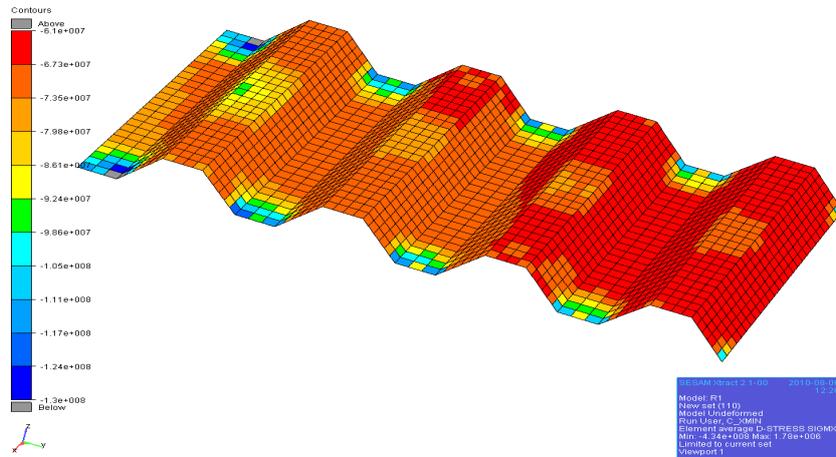
Fig. 12. Representative panel piece for the shell plating of the pontoon.

The parametric study is carried out for the part of the top plating between two transverse web frames in the mid-section of the sub-model, see Fig. 12. The sub-model in Fig. 13 consists of five sections as a conclusion of the model size sensitivity study. Part of the top plating possessing the highest overall and local compressive and tensile stresses was chosen to use as a reference panel in the parametric study as a representative panel area for the whole shell plating of the sub-model.
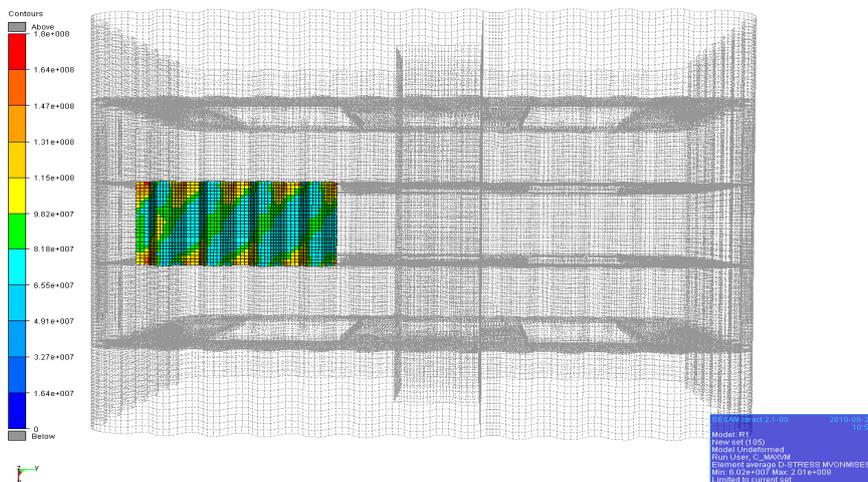
Fig. 13. Complete model with five sections and the panel piece.

The width of the panel area was decided upon in order to include a sufficient number of corrugations to prevent the stiffness values from being underestimated. The panel width (B = 5.12 m) was chosen as a value to be wide enough to include a number of between three and eight corrugations on the studied panel. A concern was to choose a panel area that would be representative enough with regard to stress distributions for the whole shell plating.

6.4. Boundary conditions

The edges of the five-section model in Fig. 8 were coupled to the global pontoon using SUBMOD. The boundaries of the submodels were subjected to prescribed displacements corresponding to the displacements of the global model for the different load cases. Since the stiffness in the longitudinal direction (D_x), is much greater than stiffness in the transverse direction (D_y) and the analyzed four-corrugation-panel breadth is greater than the four-corrugation-panel length, the restraint of the edges at y = 0 and y = B has little influence on the buckling stress.
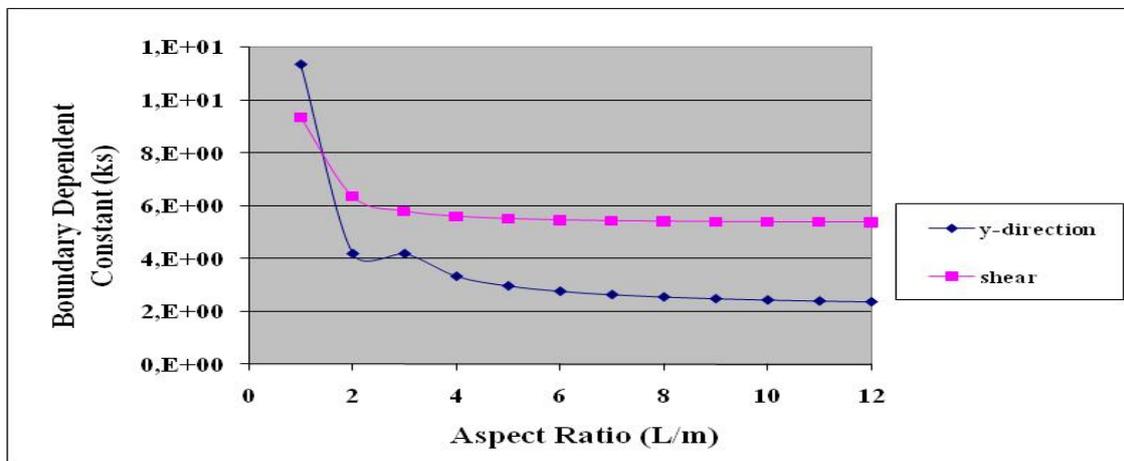
Fig. 14. The influence of aspect ratio on boundary dependent constant.

The influences of the boundary conditions from the edges of the panel to the strength values are investigated. In Fig. 14, the influence of the aspect ratio to a boundary-dependent constant for buckling due to shear stress and transverse compressive stress has been investigated. The length of the panel was set fixed, while the short plate edge of the panel varied. The experience in the parametric study showed that the possible value for the aspect ratio varies between 4.5 and 6. Therefore, it can be concluded that the length of the short plate edge (for this design) has a negligible influence on the boundary condition of the panel in question. For conservativeness the boundary conditions were assumed to be simple-supported from the edges.

6.5. The extraction of response stresses from the FE-analysis

The parametric study involved nine stress unknowns. An FE analysis of a submodel of the corrugated shell panel was used to extract these input stresses. However, these call for an iterative process, since the input stresses would differ due to the corrugation geometry being modified. Here, an iterative process is referred to using unknown stresses as an input to the parametric study from which the corrugated panel geometry is proposed. The iterative process ends when the model failure capacity is fully utilized.

The unknowns for the formulation for the buckling strength assessment are illustrated in Fig. 15 and Fig 16.
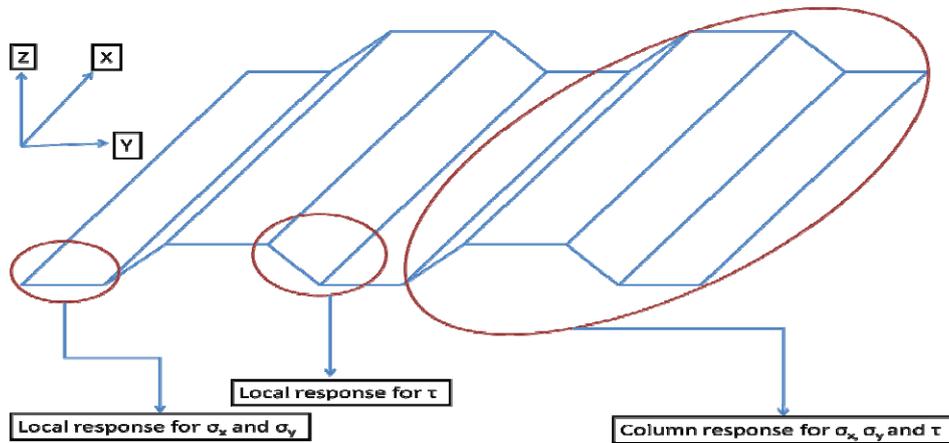
Fig. 15. Coordinate systems and response stress locating positions.

Local buckling capacity is highly dependent on the ratio of the edge stresses. A minimum and maximum of membrane stresses are used for the calculation of this ratio. Several cases for the calculation of the membrane stresses are presented in the ABS guide because membrane stresses are classified into two components; in-plane bending stresses and in-plane compression stresses. The response stress distributions in the x and y directions are established for an area that would be large enough to include at least one buckle, see Fig. 15. Therefore, the stresses were noted down for a quadrate including a buckle and the stress distributions were formed in the axial directions. An in-plane shear stress value was attained accordingly, see Fig 16.

For the maximum compressive stress in the corrugation direction required for assessing the beam-column buckling strength according to the ABS [7], the GVA-C methodology [19] is employed. This methodology suggests the usage of the highest stress value of the 70 percent of the elements over an area including a unit corrugation buckle. For the compressive stresses to be used in global buckling, average values were used as suggested in the ABS [7].

$$\sigma_{xmax} = \sigma_{ax} + \sigma_{bx}$$
$$\sigma_{xmin} = \sigma_{ax} - \sigma_{bx}$$
$$\sigma_{ymax} = \sigma_{ay} + \sigma_{by}$$
$$\sigma_{ymin} = \sigma_{ay} - \sigma_{by}$$
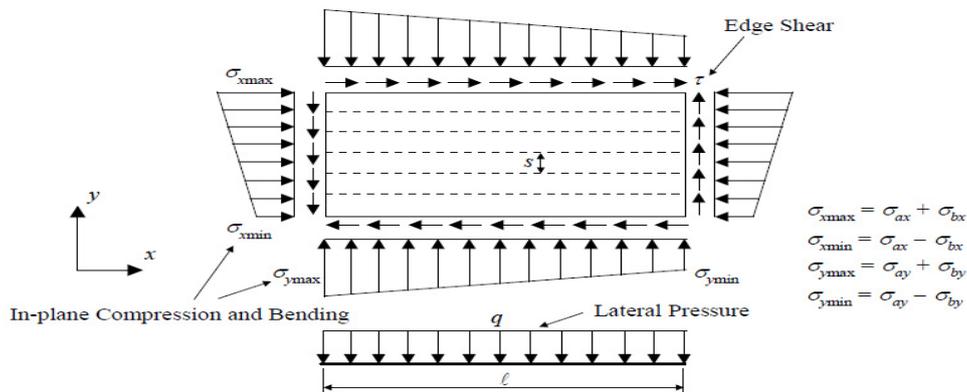
Fig. 16. Primary loads and load effects on plate according to the ABS [7].

The GVA-C methodology divides the structure into various sections and the strength assessment is made for each of these areas and thus the thickness might differ over a panel. It should be noted that the area that bears the highest stresses are used to obtain the stresses. In

this case, for the axial stresses, the plate closest to the side shell plating (furthest to the bulkhead) and for shear stresses the first corrugation web closest to the side shell plating have been used for local stresses. This area had the highest stresses because it was located furthest from the longitudinal bulkhead, which attracts more stresses compared to the other part of the shell plating. This phenomenon is called shear lag effect. Longitudinal bulkheads and side shells in the original design are about equally shear stiff. However, when the shell plating is converted to corrugated panels the longitudinal bulkhead is expected to bear a higher degree of the shear forces inherent in the shell plating. This is due to the reason that corrugated panels are not as stiff as flat panels in shear.

6.6. An FE-analysis of the initial corrugated model

Response stresses from the initial corrugated model in Fig. 17 were used as input values to the parametric study. The geometrical properties were calculated with the condition that the section is thin-walled and the thickness is small. The geometrical and strength characteristics of the initial model can be found in Appendix D.

Features

B = 5120 mm
L = 2560 mm
a = 320 mm
b = 320 mm
c = 536 mm
d = 430 mm
s = 1280 mm
t = 19 mm

Stress response

σ_{zmin} = 81.46 MPa
σ_{zmax} = 02.48 MPa
σ_{ymin} = 06.63 MPa
σ_{ymax} = 20.07 MPa
Tau = 70.40 MPa
σ_a = 82.54 MPa
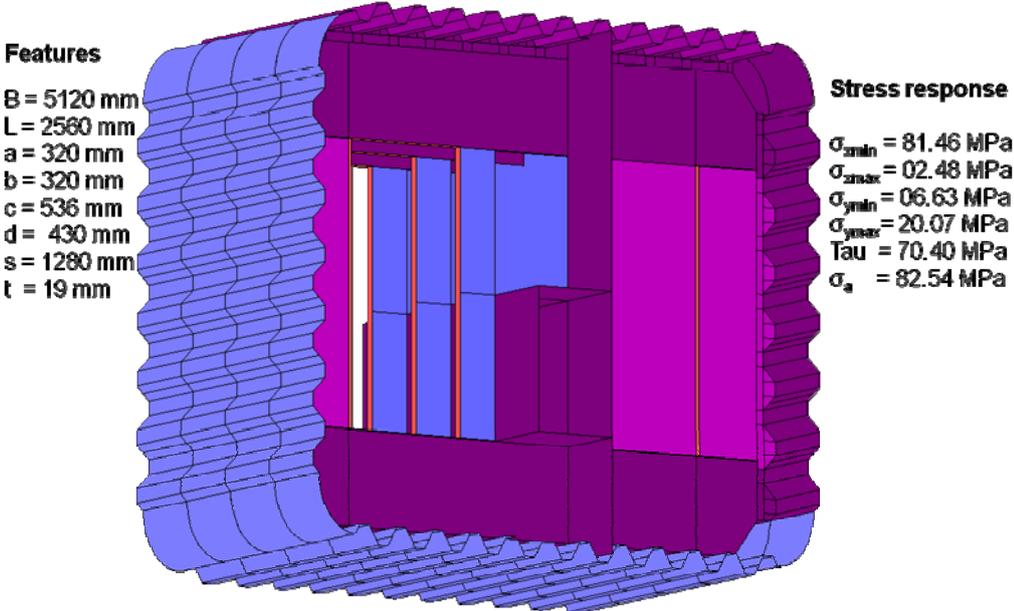
Fig. 17. Initial corrugated model considered for analysis.

As expected using the structure in Fig. 17, the stresses in the transverse direction are considerably smaller compared to the longitudinal stresses. The reason is that the structure is well supported in the transverse direction by the frames and that the corrugation as such is very flexible, thus making stiffness low compared to the web frames. These stresses are of a compressive nature. The geometrical and strength characteristics of the initial corrugated model can be found in Appendix D.

6.7. Single variation of parameters

The following seven values were checked during each of the iteration processes.

1) Local buckling capacity.
2) Unit corrugation buckling capacity.
3) Overall buckling capacity.
4) Ultimate strength capacity of the plate under combined in-plane stresses.
5) Ultimate strength capacity of the plate under lateral load and with in-plane stresses.
6) Weight reduction in shell plating (compared to the stiffened model).
7) The von Mises criterion (not higher than 90 percent of yield stress).

Figure F2 illustrates how each of the corrugated cross-section parameters influence the local buckling capacity. The widest plate of the cross section was denoted "m" and all the buckling and ultimate strength assessments and aspect ratio calculations were made with this value. Figure 18 illustrates the transition of critical plates of the cross section. Depending on different upper flange widths, 'm' first follows 'b' until m = 320 mm and between 320 and 600, the value of 'm' is assigned to 'c'.
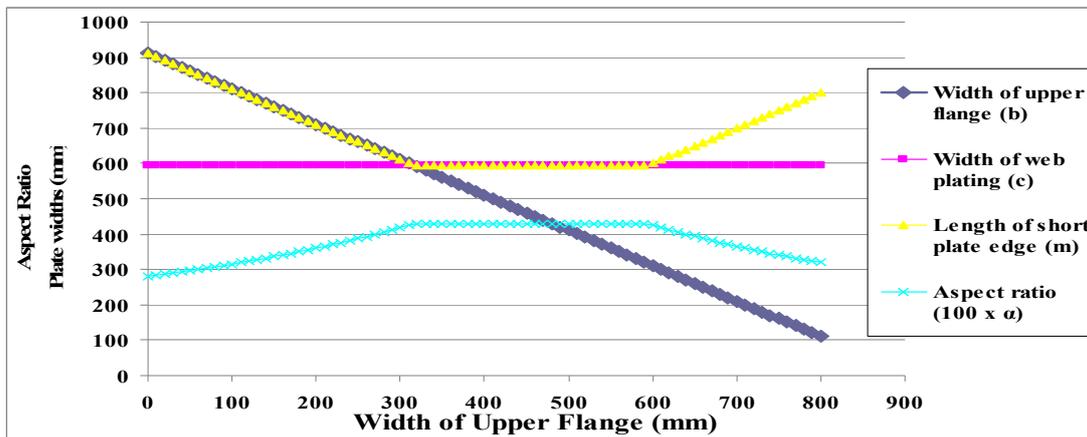
Fig. 18. Procedure for choosing a critical plate strip of the corrugated panel.

The widest plate strip in the cross section will be the most critical one with regard to local buckling. Thus, the widest plate in the upper flange, denoted as 'm', the lower flange and the corrugation web was used to assess the local buckling strength; see Appendix H1.

Based on the above explained study, the maximum efficiency of a corrugated panel can be achieved in the following ways,

As seen in Fig. 19, a decrease in section modulus due to an increase in angle results in a higher bending stress. For constant corrugation height, a higher corrugation angle implies a shorter web plating width (c), which in turn results in a lower moment of inertia. Strength requires deep trough corrugation with a rectangular profile, but weight is favored by the opposite. Therefore, to achieve a good balance between strength and weight, a corrugation angle of 57° was used as the most efficient value throughout the parametric study. This value was the lowest allowable corrugation angle according to the ABS criteria [7].

24
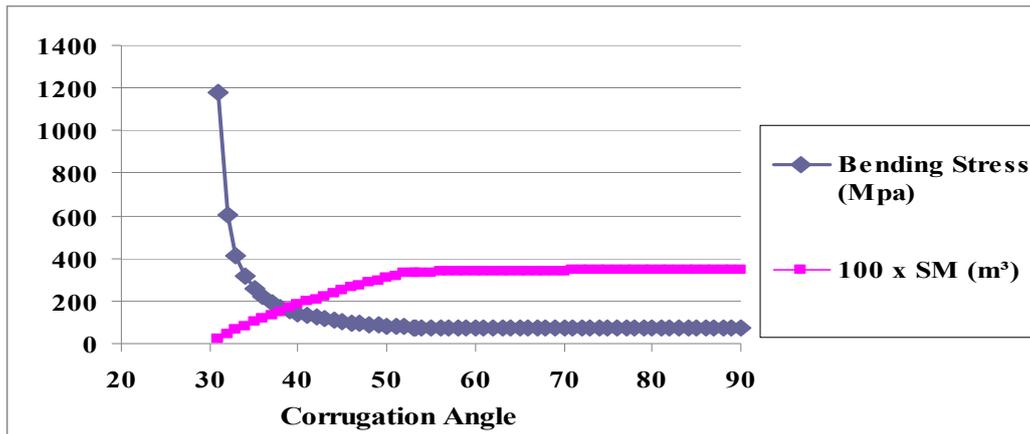
Fig. 19. Influence of corrugation angle on bending stress.

The moment of inertia of a structure determines the stiffness of a structural member. Corrugated cross sections can be utilized for lightweight structures by locating as much section area as possible away from the neutral axis.
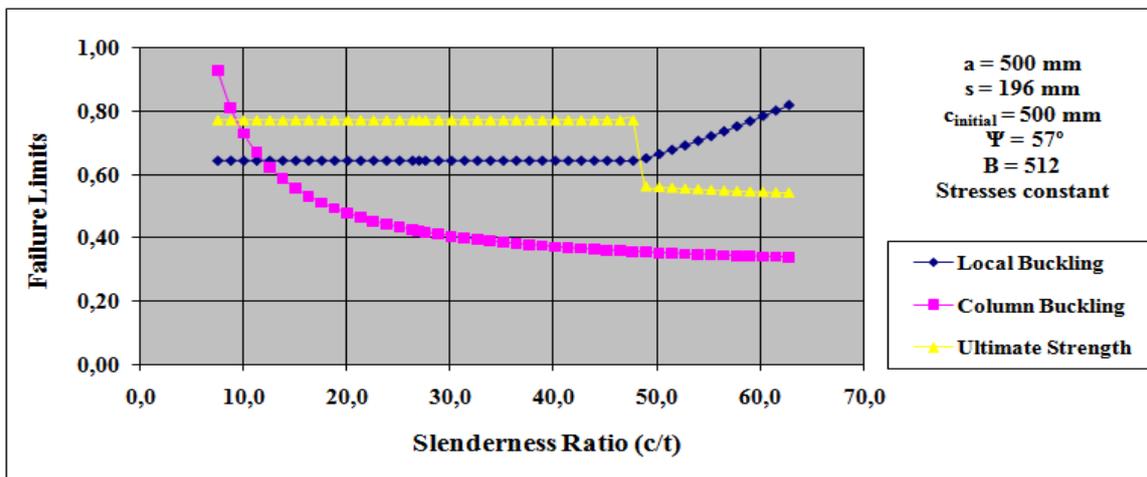
Fig. 20. Influence of slenderness ratio to different limit states.

Figure 20 illustrates the influence of the slenderness of the web plating to different failure limits. The transition of the failure criteria from ultimate strength to local buckling is also seen in the graph. This figure was also employed during the design process of the first proposal presented in Chapter 7. The stability of the plating depends on the slenderness. As the slenderness of the web plating increases (from 50 to 63), the local buckling capacity is exhausted linearly (see Fig. 20). However, for this structure, the web plating does not become critical with regard to local buckling for values below 500 mm. This is because the lower flange width is the most critical member in the cross-section, which determines the local buckling capacity. This is why the local buckling capacity is constant for values under 50 for the web plating, while the ultimate strength is the critical design criteria. Therefore, as seen in Fig. 20, when the web plating becomes the widest of all the plate strips a local buckling limit suddenly starts increasing. However, higher slenderness ratios are favorable for the beam capacity to resist beam-column buckling. The ultimate strength of the structure remained constant in Fig. 20 until $c/t = 47$, after which the ultimate strength capacity of the web plating suddenly drops due to critical value of the slenderness factor.

6.8. Combined variation and derivation of the final scantlings

Four parameters: the width of the upper flange, the height of the web plating, the width of the unit corrugation and the corrugation angle (a, d, s and Φ) were used for the combined iterative variation of the parameters. Each parameter has been varied together with another parameter. Their values were bounded with lower and upper limits and calculations for each buckling failure and ultimate strength criteria were made for cases when both of the parameters were increasing and when one parameter is increasing while the other one is decreasing in the specified boundaries. As a result, 18 different combinations were made and for each combination five strength criteria and weight reductions were checked to see if the structure passed the test or not. The idea was to extract one geometry for each of the combinations. Finally, among the proposals obtained one of the designs was selected. Based on the single variation of the parameters, which had been previously carried out, the varied parameters were slightly altered to gain more weight reduction or to increase strength without losing the weight benefit obtained. The reason is that the proposed geometry would still have some margin of error and thus some improvement could be found from the graphs and the margin to failure could be exploited to reduce the weight further. Sometimes the variation of parameters would not influence the failure mode, which was critical for the design in question.

A three-dimensional diagram in Fig. 21 is formed for better comprehension of the influences of the variations. It shows an example of the variation of corrugation height and upper flange width together with a local buckling check on the z-axis.
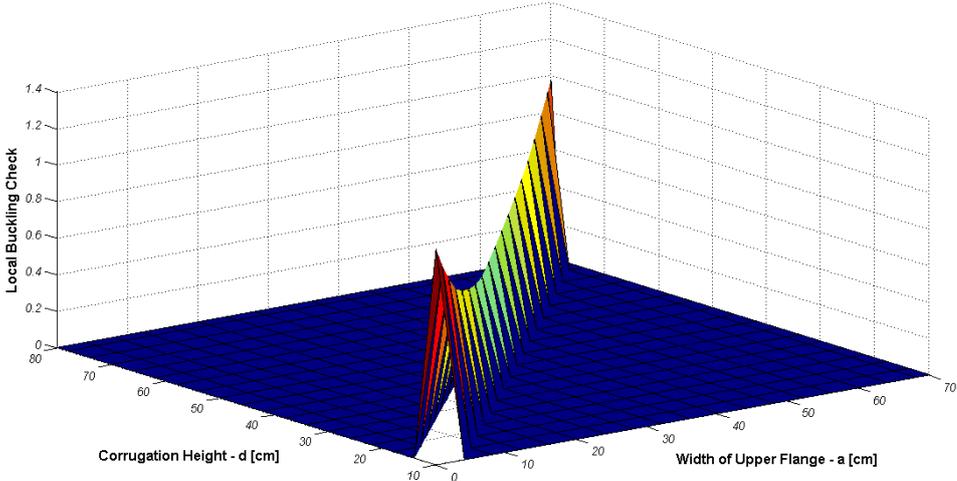
Fig. 21. Influence of corrugation height and flange width to local buckling limit state.

The analytical study has demonstrated that the influence of the geometry of the corrugation profiles on the buckling behavior of the corrugated shell plating along with the application of the ultimate strength criteria under combined in-plane stresses and lateral loads can be significant. Figure 21 shows that there is a sharp optimum along the diagonal from a low height and flange width to large values of both width of the upper flange, a, and the corrugation height, d. The values of a and d have been chosen in a way so that an optimum minimum can be achieved with respect to the local buckling strength according to the ABS [7].

7. Verification of results from parametric study

Two alternative designs are chosen from these proposals and analyzed with FEM. After a systematic variation of all the defined corrugation parameters, six different designs, all of them having unequal flanges, were derived. As a conclusion, the best geometry among them with regard to weight was chosen for an FE-analysis. For different design considerations around 12 analyses were carried out.

7.1. Analysis of asymmetric corrugation proposal

Using the response stresses from the initial corrugated model, a parametric study has been carried out.

As seen from Table 8, this structure has exceeded its local buckling capacity by 7 percent on iteration 1. Therefore, the widest plate strip (b) could be decreased. However, the ultimate strength criterion, which is dependent on the slenderness ratio of the plate, was very close to failure. If the plate width is decreased in order to recover the structure from the local buckling failure, the critical buckling stress in the longitudinal direction exceeds the ultimate strength of the plate with respect to uni-axial stress. This is not allowed according to ABS rules.

Table 8. Stress responses for an asymmetric corrugation proposal.

Iteration	Response stress	Weight reduction (%)	Action	Failure mode (local buckling)
Initial	82 MPa	27	a=320mm b=320mm d=430mm	On both flanges 48%
Iteration 1	162 MPa	39	a=740mm b=920mm d=230mm	On lower flange 107%
Iteration 2 (Final)	153 MPa	38	a=740mm b=920mm d=260mm	On lower flange 97%
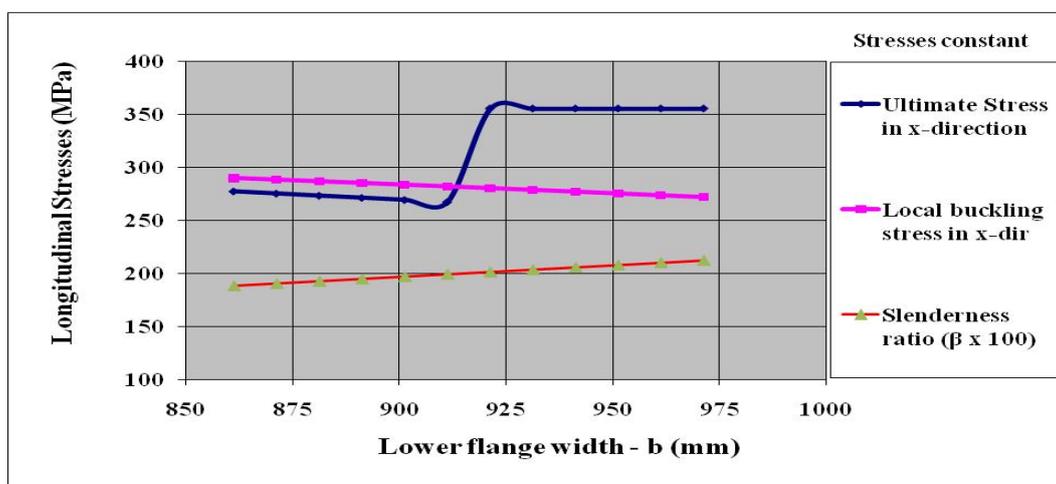
Fig. 22. Influence of lower flange width for stresses in the x-direction and slenderness ratio.

The slenderness ratio was '2.02' for this structure in iteration 1 and the limit value for slenderness ratio is '2' as seen in Fig. 22 according to the ABS. Figure 22 illustrates the

sudden increase in ultimate stress when the slenderness ratio passes the critical limit of '2' To avoid a failure of meeting the ultimate strength criteria while utilizing the structure for local buckling, a variation in the cross section was to be made without decreasing the flange width. Through this, the web height was increased in order to favor shear stress. By doing so, the slenderness ratio would be kept above the value of '2' because the widest plate strip (b) is not changed. As a result, the height of the web plating was increased by 30 mm as presented in Table 8.

The final geometry has passed all the criteria according to the ABS and we concluded with a 32 percent weight reduction compared to the stiffened panel. Figure 23 is the deformed view of the final corrugated panel. The critical failure mode is local buckling on the lower flange. Further details of this model can be found in Appendix D.
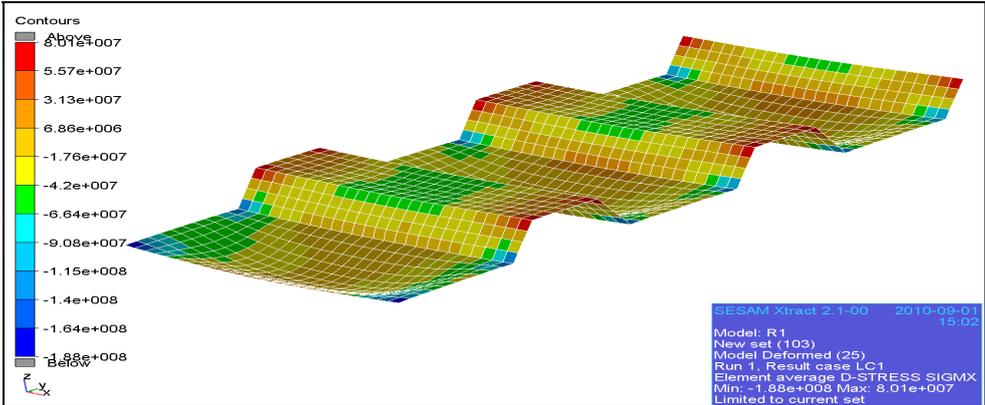
Fig. 23. Deformed FEA view of the final design (units in MPa).

7.2. Analysis of the symmetric corrugation proposal

It was of interest to continue the study with another type of corrugated shell plating displaying equally or better strength characteristics. The first proposed design was known to be geometrically different from the corrugation types employed in the industry, for example, considering the fact that bulkheads with equal flange widths for tankers have a similar design loading to that of the shell plating of the pontoon. Corrugations with equal flanges would also result in robustness in manufacturing. Also, the structure can take lateral loads from both sides of the structure unlike the corrugated panels with unequal flanges. Therefore, a design with equal flanges was aimed to be made. Another interesting factor was to look for lower thickness values, since the thickness has always been kept constant for the previous designs (19 mm, as in a stiffened model). The idea was to modify the corrugations mainly by decreasing the plate thickness without making significant changes in the flanges and web height. Strength and geometrical details of the first iteration can be found in Appendix D.

Table 9. Stress responses for a symmetric corrugation proposal.

Iteration point	Buckling strength	Weight reduction (%)	Action	Failure mode (beam-column buckling)
Initial	325MPa	27	a=320mm b=320mm d=430mm t =19 mm	67%
Iteration 1	288 MPa	53	a=b=360mm d=430mm t =12 mm	74%
Iteration 2	275 MPa	57	a=b=360mm d=430mm t =11 mm	80%
Iteration 3 (Final)	289 MPa	59	a=b=450mm d=370mm t =11 mm	91%

After the first iteration, the upper and lower flange widths along with the height of the corrugations were to be varied in order to find the lightest structure. Figure F5 was one of the figures from the parametric study that was created to decide on the next iteration to be modeled. The flange width and the minimum corrugation height were chosen based on this figure.

The design process concluded with a corrugated shell structure with a plate thickness of 11 mm and equal flange widths (see Table 9).

Beam-column buckling has turned out to be the governing design criteria for this structure. A further decrease of the corrugation height would lead to failure so the design process was ended at the third final iteration. Geometrical details of the final design are given in Appendix D. Figure 25 shows a deformed view of the final proposal.
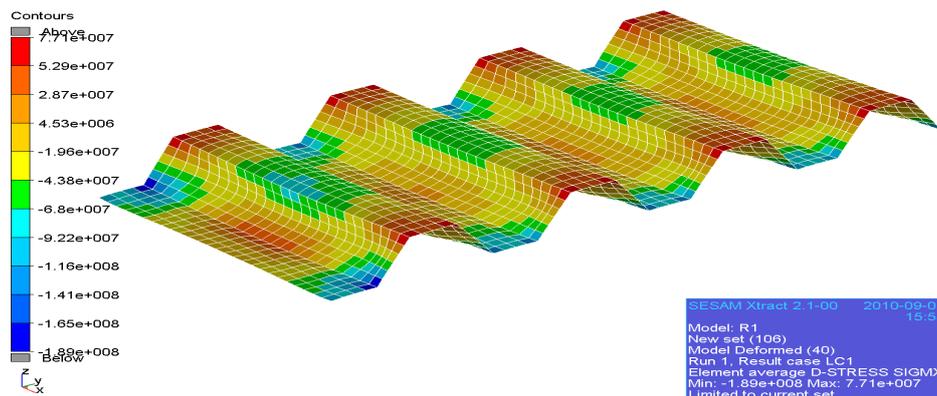
Fig. 25. Deformed FEA view of the final design (units in MPa).

The weight reduction was found to be very sensitive to the plate thickness (see Fig. F6) and therefore the weight reduction of this design was higher than that of the first design proposal.

29

7.3. Simplified fatigue analysis

The level of sophistication required in the analysis was as specified in the ABS rules for offshore structures [24]. Rules for structural modeling and boundary conditions and the considered loads and load combinations are considered. Reference figures can be found in Appendix B. Table 10 shows fatigue test results for the two proposals.

Table 10. Analysis of the corrugated shell plating for fatigue test.

Model	Plate thickness	Principle stress range (MPa)	Maximum allowable P stress	Result
Proposal 1	19 mm	19.01 to 29.15	98 MPa	pass
Proposal 2	11 mm	20.22 to 31.2	98 MPa	pass

The following results can be commented from the fatigue analysis:

1. The bottom left bilge was experiencing more stress; see Appendix B.
2. As FDF was used as 3, the ranges showed values quite far from the maximum allowable principal fatigue stress [24].
3. Fatigue strength criteria of the shell plating of the structure were not applied in the parametric study. Therefore, the structure was not modified to improve the resistance of structure to fatigue. This is because it was presumed that the fatigue is of secondary importance for the structure in question.

8. Additional studies

8.1. Modification of the reference model

Until this point, two different models of a pontoon part with corrugated shell plating have been proposed. Both proposals are considerably lighter compared to the initial reference model. However, it was not correct to generally favor corrugated shell plating over stiffened plating. If the stiffened model is modified in the same way as a corrugated model and general conclusions regarding a modified model are lighter than the proposed corrugated models, it would be more meaningful in the study to assess the qualities of the corrugated structures in general. This study would also contribute to our understanding of dominating design criteria for stiffened structures subjected to high lateral loads and might be beneficial to the GVA-C commercially.

8.1.1. Procedure and FEA

ABS buckling software (StruProg) was used to assess the strength characteristics of the stiffened model.

The GVA-C uses StruProg for a buckling check of the panels. It is a computerized semi-analytical model based on a recognized non-linear plate theory. It assesses the elastic buckling stresses and ultimate load bearing capacities under combined loads. Basically, the software requires input values which are compressive and tensional stresses in each direction and calculates the strength characteristics. A StruProg output sheet for the final modified stiffened structure is given in Appendix G. The post-processing of the stiffened shell plating was done similarly to the procedure followed for corrugated shell plating designs. Attention was given when using the same strength utilization and load factors that are used in the corrugated model.

Stiffened plates in real structures can be loaded under a combination of in-plane and out-of-plane loading. In-plane loads can include axial or biaxial compression and in-plane shear. Out-of-plane loading includes lateral pressure or bending about the transverse and longitudinal axes of the stiffened plate.

The following criteria were used:

i. Plate buckling control	v. Flexural-torsional buckling limit
ii. Ultimate strength of the plate	vi. Plate yield control
iii. US of the plate under lateral load	vii. Stiffener yield check
iv. Beam-column buckling state limit	viii. Stiffness of stiffener webs

At the third FEA of three subsequent designs a final stiffened model was achieved. As a first step the thickness of the initial model was decreased. Secondly, the stiffener dimensions and spacing were utilized. The flow of modification details are presented in Table 11. 12 mm of shell plating thickness (previously 19 mm) was achieved in the second iteration. Stresses from this design showed that this value was the failure limit for the plate.

As seen from Table 11, local buckling has become the designing failure mode for 12 mm thickness of the shell plating. Considering that half the weight of the structure was due to stiffeners, it was decided to continue with lightening the stiffeners. This way, the structure could become lighter. The weight of the stiffened panel, which is in the local buckling failure

limit, can be achieved only by achieving compensation between the plate thickness and the stiffeners. Hereby, the remaining capacity for the beam-column buckling limit is utilized by lightening the stiffeners (see Appendix E) and increasing the plate thickness by 1 mm. As presented in Table 11, this modification fully utilized the beam-column buckling capacity of the shell plating with the stresses extracted from the FE-analysis. Also, the increase in plate thickness recovered some of the local buckling capacity of the plate.

Table 11. Iteration flow of achieving the lightened stiffened model.

Component	Limit value (1st model)	Limit value (2nd model)	Limit value (3rd model)	Required value
Plate - buckling	0.49	0.78	0.71	0.80
Plate - ultimate	0.47	0.69	0.66	0.80
Plate - lateral load	0.25	0.63	0.54	0.80
Beam - column buckling	0.41	0.38	0.80	0.80
Flexural- torsional buckling	0.31	0.28	0.32	0.80
Plate yield control	0.43	0.33	0.33	0.90
Stiffener yield check	0.47 & 0.36	0.39 & 0.33	0.45 & 0.59	0.90
Stiffness of web	25	25	19	20.5
Thickness (mm)	19	12	13	-
Stiffener dimension (mm)	430 x 15	430 x 15	260 x 12	-
Weight reduction (%)	0	20	32	-

The flexural-torsional buckling capacity of the stiffened panel is very high compared to the Euler Buckling capacity, (see Table 11). This is favorable because the load capacity after failure is known to fall very sharply for this failure mode, whereas Euler buckling is expected to have a better post-buckling ability.
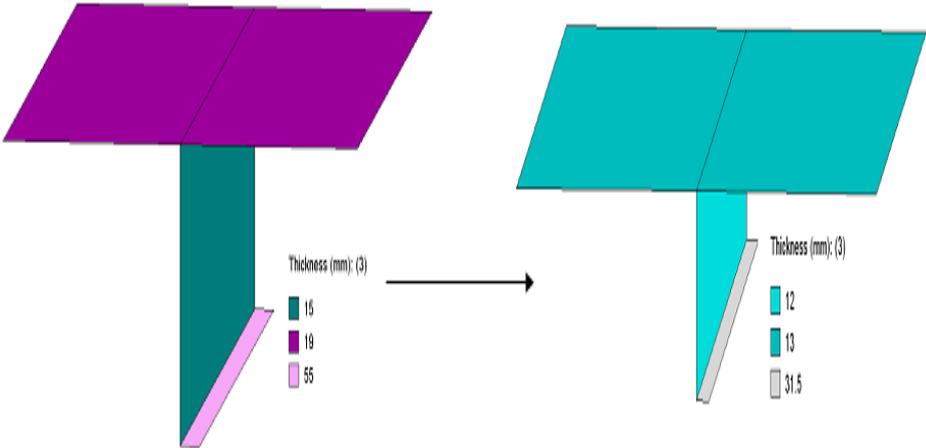
Fig. 26. Stiffener modification – existing design (left) and final design (right).

In Appendix E, the geometrical details of the stiffeners for the existing design and the final design can be found. In Fig. 26, it is shown how shell plating and stiffener thicknesses were changed. As a result, the study concluded with the 32 percent weight reduction of the existing

stiffened model. Therefore, the final corrugated design was estimated to be 40 percent lighter compared to the final stiffened model.

8.2. Depth study

The semi-submersible is going to be one of the deepest platforms in the world. The design process for the pontoon part is carried out for a depth of 30 meters. At this depth, bending stresses due to lateral load are considerably high. At different depths, governing design criteria (e.g. buckling, ULS) might differ or the employment of corrugated shell plating might not be advantageous at all. Although the designing failure mode implies buckling for loads at 30 meters, it is of interest to generalize the strength characteristics of the structure for different operating depths of the pontoon.

A second alternative design with a corrugated shell structure is used for this study. Lateral loads for operating depths of 20 m, 10 m and 0 m are applied to the structure. Results for the 30 meter depths were already at hand. The cross-section properties were kept constant; only the plate thickness of the shell plating of the structure was modified for each depth. The study was repeated also for the optimized stiffened model so that a comparison could be made with regard to the weight reduction potential for both designs and the failure modes. The results for the optimized stiffened model are given in Chapter 8.

For each depth, the thicknesses were decreased until the shell plating fails by local or beam-column buckling. An iterative process was employed for finding the final thicknesses. Figure 27 illustrates the final thicknesses of the corrugated and stiffened panels for each water depth of the pontoon.
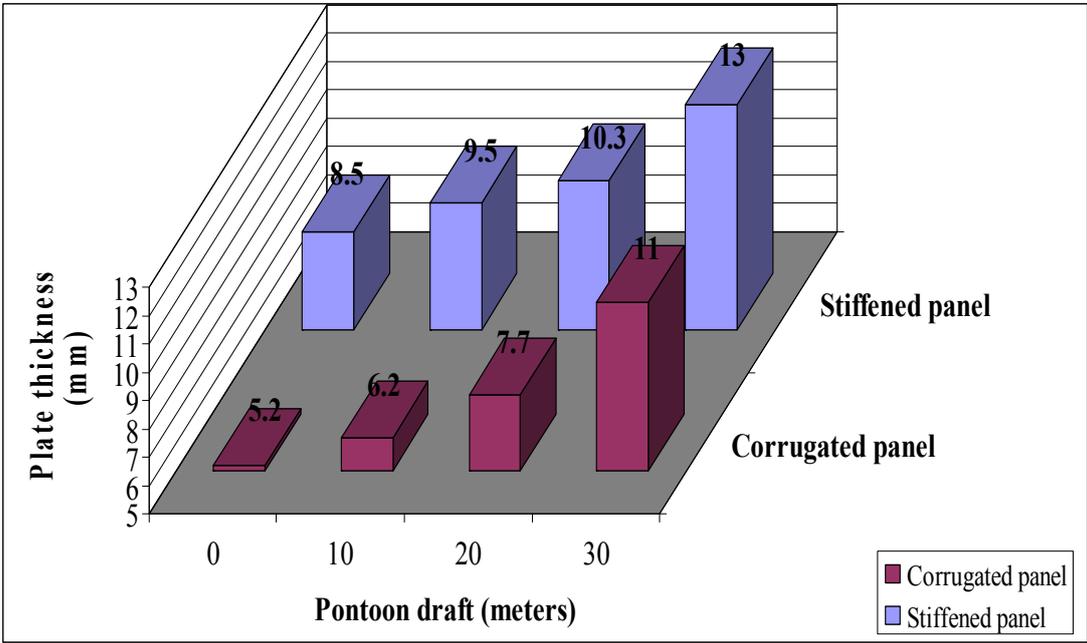
Fig. 27. Final shell plate thicknesses for different operating depths.

As seen in Fig. 27, for the stiffened model the thickness could be decreased by 34 percent between 0 and 30 meters, while the corrugated structure allowed for a 50 percent decrease in shell plate thickness. It was observed that as the pontoons get deeper, due to the increase in bending stresses because of lateral load, the governing design criteria shift from local

buckling to beam-column buckling. The failure modes for each of the structures for different depths are given in Table 12. The thickness increase between 20-30 meters is around 33 percent, while it is 15 percent between 0 and 10 meters. This is because the beam-column buckling limit state is less sensitive to plate thickness compared to local buckling, thus requiring a higher plate thickness increase as the pontoon gets deeper.

Table 12. Failure modes of the pontoon shell plating for different operating depths.

	Pontoon depth	0 m	10 m	20 m	30 m
Failure modes	**Stiffened**	Local buckling	Local buckling	Local buckling	Column buckling
	Corrugated	Local buckling	Local buckling	Column buckling	Column buckling

Ultimate strength was not experienced for any water depth. Buckling was the dominating failure mode. It is interesting to see in Table 12 that the corrugated structure fails with regard to beam-column buckling somewhere between the 10-20 meter water depths, while for a stiffened structure this is between 20-30 meters. Therefore, it was required to increase the shell plate thickness for a corrugated structure at a lesser depth level than the stiffened structure with reference to the reason explained in the previous paragraph. Hence, the total weight of the stiffened pontoon structure approaches the weight of the corrugated pontoon structure as the water depths increases. This can be seen in Fig. 28.
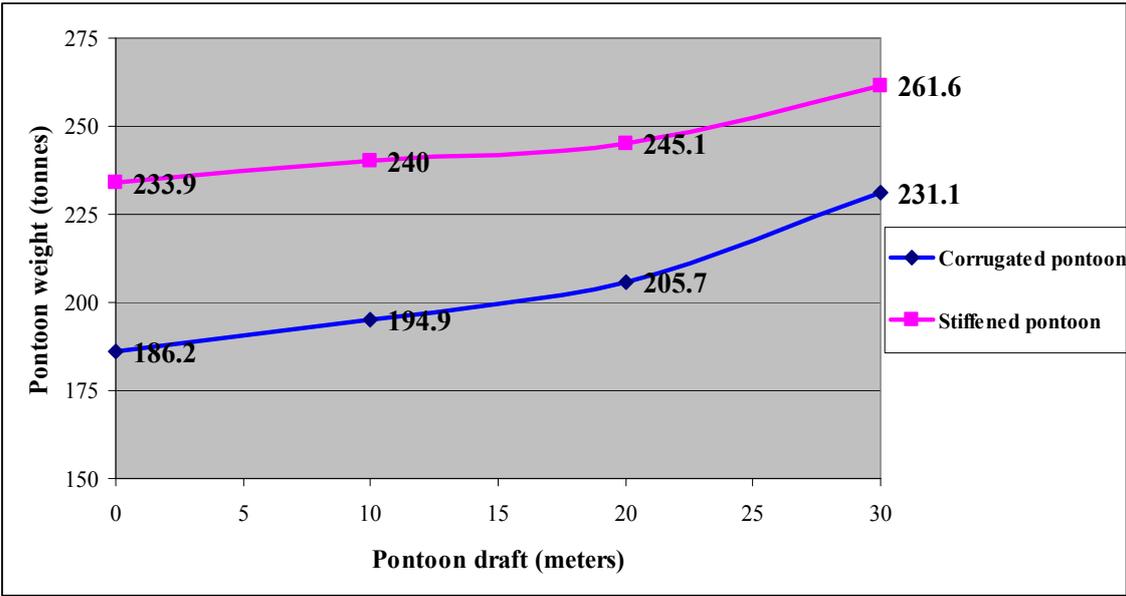
Fig. 28. Weight comparison of corrugated and reference pontoon at different drafts.

The weight given in Fig. 28 is the total weight of the pontoon part. This includes not only the shell plating but also other structural members, such as transverse web frames, trunks, access tunnels and cross-section plating. The weight reduction of the pontoon varies from 20.4 percent at 0 meters to 11.7 percent at 30 meters.

34

9. Manufacturing and cost analysis

A main drawback for this kind of geometry is constructional complexity. This will require considerable initial investment and a skilled operator for the bending procedure of the panel. Figure 29 shows an example of a bending machine that can be useful for implementing a corrugation profile on a flat plate. On the other hand, there will be a weight and cost benefit due to the exclusion of stiffeners for shell plating. Moreover, there will be a reduction in welding, painting and manufacturing time.

Fig. 29. A hydraulic press-brake plate bending machine in operation.

9.1. Assumptions and restrictions

The following assumptions are valid for the analysis:

- The product will operate for 25 years without docking.
- The process only shuts down at the end of a shift and for bath replacement.
- All weldable structures were valid for welding type SMAW.
- Shell plate panels were considered to be jointless in the transverse direction.
- The steel-cutting process was not considered.
- The assigned prices were assumed only for the purpose of comparison.

9.2. Manufacturing fact

Corrugated shell plating requires the bending of flat plate panels resulting in a radius instead of a welded joint between the corrugated web and flange. Therefore, the influence of the radius was checked by FEM and was found negligible as is seen in Table 13.

Table 13. Stress response from different model sizes.

	σ_{ymin} (membrane stress)	σ_{xmin} (membrane stress)	**Shear stress**
With radius	98.0 MPa	68.3 MPa	79.5 MPa
Without radius	97.6 MPa	65.8 MPa	79.0 MPa

9.3. Savings associated

The savings that can be readily observed without any numerical calculation are welding, painting and man-hours. A corrugated panel precludes welding materials associated with stiffener attachment to the main plate. Only end-joint butt welding is valid in this case. As for painting, without the presence of stiffeners, the corrugated panel comprises a larger surface area exposed for painting. Hence, it saves a painting-associated material cost. Overall, the man-hours needed for performing this stiffener attachment and stiffener painting is exempted, and, through this, any cost and time involved in this work will be saved.

9.4. Comparison

The present work has given an emphasis to a comparative investigation of two panel forms, for example stiffened and corrugated. Although some aspects of these panel forms have been studied individually by different authors, this work presumably presents a comparative investigation of its kind for the first time. The analysis was made on a portion of the cross-section for computational efficiency. Two parameters, namely thickness and height, were varied in order to check the effect of stresses on the pontoon weight and consequently the production cost. Figure 30 depicts the thickness influence on the production cost. It is evidently clear that corrugated panels are cost-effective.
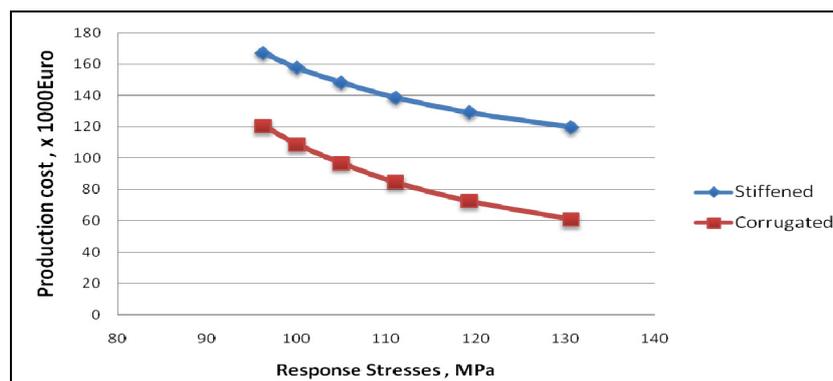
Fig. 30. Production cost versus stress response due to thickness variation.

The second parameter varied was corrugation height. In order to investigate the effect of corrugation height on the production cost, several FEAs were carried out for web heights in a range of 230 mm and 430 mm. A higher value of corrugation web causes a larger shell plating surface, thus increasing production costs. In order to assess the range of production costs for the variation of corrugation height, a graph was plotted, see Fig. 31, with production costs against response stresses obtained from the FEA.
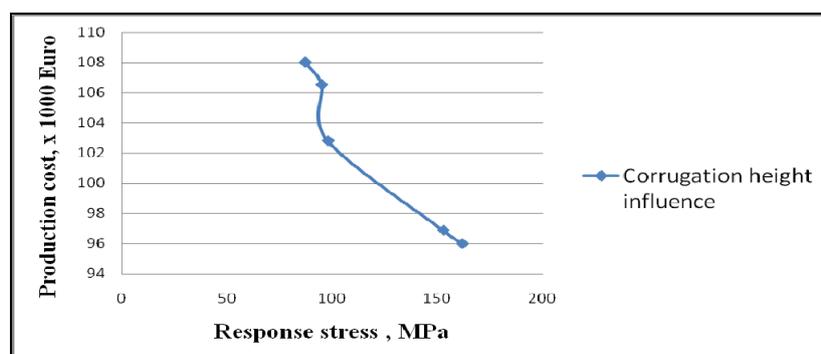
Fig. 31. Production cost investigation for height variation.

36

In Appendix J, a cost model was prepared to validate production costs with respect to varying plate thickness and corrugation height. For this purpose, an existing cost model [9] was modified in terms of a substantial update and a new calculation part for the cost of painting. Assumed values can be seen in Table 14.

Table 14. Assumed values for cost analysis for different cost components.

Cost	Value	Unit
P_a (steel cost)	800	Euro/ton
P_s (operator cost)	10	Euro/hour
P_{pc} (paint cost)	5	Euro/liter
P_{wc} (welding consumables)	2	Euro/liter

On the basis of the comparative cost evaluation, finally, the cost reduction becomes 35 percent for the one proposed that dealt with an unequal flange width; see Table 15.

Table 15. Cost obtained for corrugation height variation.

| Corrugation height | Corrugated | |
	Cost shell (% reduction)	Total cost (% reduction)
230 mm	96 (43 %)	140 (34 %)
260 mm	97 (42 %)	141 (33 %)
310 mm	103 (38 %)	147 (30 %)
350 mm	107 (36 %)	151 (28 %)
370 mm	108 (35 %)	152 (28 %)
430 mm	114 (32 %)	158 (25 %)

On the other hand, the second proposal with an equal flange resulted in a 49 percent production cost reduction; see Table 16.

Table 16. Cost obtained for thickness variation in Euros (stated in thousands).

| Thickness | Stiffened | | Corrugated | |
	Cost shell (% reduction)	Cost total (% reduction)	Cost shell (% reduction)	Cost total (% reduction)
9 mm	120 (28 %)	164 (22 %)	61 (64 %)	105 (50 %)
11mm	129 (23 %)	173 (18 %)	73 (56 %)	117 (45 %)
13 mm	139 (17 %)	183 (13 %)	85 (49 %)	129 (39 %)
15mm	148 (14 %)	192 (9 %)	97 (42 %)	141 (33 %)
17mm	158 (5 %)	202 (4 %)	109 (35 %)	153 (28 %)
19 mm	167 (reference)	211 (reference)	121 (28 %)	165 (22 %)

The production cost was also validated for total pontoon structure production. In this case, it was 28 percent and 39 percent, respectively, for the unequal and equal flange proposals. For comparison, the production of stiffened shell plated pontoon was calculated. The production cost of modified final stiffened pontoon was reduced by 23 percent at the shell only and 18 percent for the whole pontoon structure.

10. Summary

Table 17 summarizes weight reductions for the corrugated plating proposals with respect to the reference pontoon sections and the weight reductions for the two proposals.

Table 17. Weight comparison among the proposals, initial pontoon and modified pontoon.

Model (compared to)	Shell plate weight in tons (% reduction)	Total pontoon weight in tons (% reduction)
Initial reference stiffened model	193	342
First proposal (initial)	120 (38 %)	255 (25 %)
Second proposal (initial)	79 (59 %)	214 (37 %)
Modified stiffened pontoon (initial)	131 (32 %)	279 (18 %)
First proposal (modified)	120 (8 %)	255 (9 %)
Second proposal (modified)	79 (40 %)	214 (23 %)

Depending on the results obtained throughout the thesis work, a summary of the comparative achievements is presented in Table 18.

Table 18. Weight and production-cost reduction summary in percentage.

Model	Weight (ton) (% reduction)	Production cost (1000€)(% reduction)
Initial reference stiffened model	193	167
Modified reference stiffened model	131 (32 %)	129 (23 %)
Asymmetric flange corrugated shell proposal	120 (38 %)	108 (35 %)
Equal flange corrugated shell proposal	79 (59 %)	85 (49 %)

Therefore, in terms of cost and weight, it is validated that a corrugated shell plating is favorable compared to the stiffened shell plating. The initial reference stiffened model that is the GVA-C model was compared with a modified stiffened model that is theoretically the lightest possible sustainable structure. From this comparison, it can be concluded that the modified stiffened shell plating was even lighter than the initial stiffened reference model in terms of both weight and cost-effectiveness.

On the other hand, during the comparison, the equal flanged model dominated in every respect. Figure 33 shows a comparative graph of the weight and cost summary for the four different types of shell plating applied on the same pontoon at different times. Thus, the equal flanged corrugated shell plating is recommended based on this study.
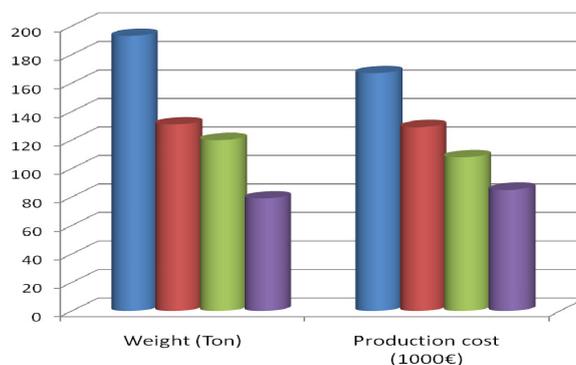
Fig. 32. Weight and production cost summary.

11. Discussion

Corrugated panels are acknowledged as great load carrying members. A promising development for lightweight design in the marine industry is the utilization of corrugated shell plating instead of continuous stiffened plates. In order to investigate the feasibility of a change of practice, this project set out to challenge the present design practice by a theoretical and numerical optimization process based on a strength criteria and an assessment of manufacturability and economy. The ultimate limit state (ULS), the fatigue limit state (FLS) and the buckling strength of a representative corrugation panel were employed, based on the rules of the ABS [7]. The response stresses of the structure were calculated by an FEA. The influence of geometric parameters on the strength was studied. The panel was designed to primarily support a lateral load and compressive stress in the longitudinal direction and shear.

The ULS was calculated for maximum response in extreme storm condition (100-year hurricane). The serviceability limit state (SLS) was not employed at all in this study. The difference in these load cases is the factors they use for the assessment of buckling and yield strength. Responses for an extreme storm condition are higher. Scanned results from numerous load cases were used to minimize the number of stress plots. Focus elements were selected based on maximum stresses from different load cases. A disadvantage of using scanned stresses is that the results are selected from many combinations of simultaneous load cases and contiguous elements may come from different snap shots. This makes it more difficult to judge the deformation behaviour of the total structure every time a geometrical parameter was changed. However, a short study of the load cases concluded that for the shell plating in question a very small number of load cases dominate the structural response. Therefore, these load cases can be used to design the structure.

Thickness is the most effective parameter among others with regard to the lightweight design of corrugated shell plating. If the column buckling is the governing failure mode, the most effective weight reduction could be achieved by reducing the thickness. If the corrugation height rather than plate thickness is decreased with the same influence on weight, the decrease in the column buckling capacity is less when thickness is changed. As long as no other criterion takes over and determines the design, one should reduce plate thickness until local buckling takes over. This was employed between the iterations.

The column buckling of the unit corrugation as a beam is expected to be the designing failure mode for this structure where the bending stresses are very high due to hydrostatic pressure. However, it was concluded that the local buckling mode, and, in some cases the ultimate strength of the plate areas, has required attention. The span of the transverse web frames is rather short for column buckling to be the dominating failure mode.

For various drafts of the production unit the shell plating of the pontoon was modified with regard to plate thickness. Therefore, minimum thicknesses were found for each depth both for the corrugated and stiffened structures. It should be noted that these minimum thicknesses cannot be employed in real life. The minimum shell plating thickness is bounded by classification rules. The main idea was to compare the weight and strength characteristics of the structure at various depths, and, therefore, this was not considered.

The buckling and ultimate strength of structural components is highly influenced by the amplitude and shape of the imperfections introduced during manufacturing, installation and transportation. These imperfections could be misalignments of joined components or initial distortion due to any fabrication-related process and/or welding. However, the FE-analysis did not incorporate these stresses while the parametric study has included the ABS rules in which these imperfections are implicitly formulated.

With a significant weight and strength balance, corrugated panels can be favourable in terms of production-cost-efficiency. The introduction of the bending machine, automatic welding and the painting machine is a good choice for fast and cheap shell plate panel construction. It can also be favourable for surveyors in the absence of major obstacles like stiffeners.

In the original structure, an air pipe extends from the pontoon level to the deck level. According to the ABS, when performing a local structural analysis, this pipe must be considered fully filled. In this study, the static pressure due to the water in the air pipe has not been considered. This pressure is an internal pressure. Obviously, when this effect is accounted for, the strength capacity of the shell plating, especially over a local region, would be less. Besides, the internal pressure from the tanks if this exists, would also introduce the buckling and ultimate strength capacity of the shell plating. Considering these internal pressure effects, an equal-flanged corrugated panel would be advantageous for withstanding lateral loads from both sides compared to the one with unequal flanges.

Dominating stresses are in the longitudinal (corrugation) direction of the panel. A corrugated panel is not as stiff in the transverse (perpendicular to the corrugations) direction. Therefore, the stresses in the transverse direction never reach critical values for dominating the design process.

12. Conclusions

The fundamental aim of this master's thesis was to explore the replacement of stiffened shell plating with corrugated shell plating. The structure should be viable in terms of structural strength and investment. Both the stiffened panel and the corrugated alternative needed optimization in order to be comparable. In the final iteration, the weight of shell plating was reduced by 59 percent for a corrugated panel and by 32 percent for a stiffened panel.

 From the analysis carried out in the study, the following conclusions are deducted:

- Buckling is the governing design criteria for the pontoon in question. Column-beam buckling of the unit corrugation is the designing failure mode.

- Local buckling occurs in the widest plate strip of the panel.

- Structural efficiency / weight ratio of the corrugated pontoon shell plating is higher than that of the stiffened shell plating for the same plate thickness and operating depth.

- High corrugation angles proved to be more efficient, for example rectangular corrugation is better than a trapezoidal or a triangular profile with an equal section modulus.

- Both designs, the stiffened panel and the corrugated alternative, demonstrate good fatigue resistance.

- The weight reduction for the total pontoon structure with a corrugated shell structure is calculated as 11.7 percent compared to the modified stiffened pontoon structure for 30 meters. For a 0 meter water depth, this value increases to 20 percent.

- The governing design criteria for the stiffened shell plating shifts from column-beam buckling to local buckling between the depths of 20-30 meters, whereas in corrugated shell plating the shifting from column-beam to local buckling occurs between 10-20 meters.

- The most optimal pontoon structure with corrugated shell plating becomes more favorable compared to the one with stiffened plating when the operating draft decreases. The reverse is true; the corrugated structure becomes less favorable compared to a stiffened structure as the depth increases due to lateral load-induced bending stresses.

- Despite having complexity in manufacturing procedure, corrugated panels show good agreement between weight reduction and production costs. It was of interest to investigate the nature of an additional exposed underwater shell plating area. Even 20 layers of coating of painting application was proved insignificant in an overall cost analysis (see Fig. 30).

13. Future work

- The study was limited to the design of pontoon shell plating. However, pontoons of the rig were designed for stiffened shell plating. It is of interest to increase the level of optimization by finding better solutions for corrugated shell plating. Therefore, the access tunnel, stiffeners in the cross section, trunks, transverse web frames and internal plating can be modified or avoided for structures with corrugated shell plating. The rig could be further lightened.

- The lightweight design of corrugated shell structures might attract a high interest in the marine industry but a detailed investigation should be carried out in order to identify the manufacturing problems in the yards due to the lower steel sheet thicknesses for corrugated alternatives.

- It is also interesting to perform a post-buckling analysis for the final corrugated designs to consider robustness.

- The span of the transverse web frames can be further increased, since they are too short for beam-column buckling to be a critical failure mode in some cases.

- The beam-column shell plating of other parts (columns, deck box, etc.) of the rig can be corrugated as the pontoon shell plating.

- A more detailed analysis can be performed to identify possible concerns regarding the manufacturing of corrugated sheets. Initial investment costs and difficulties for a yard to switch from stiffened shell plating to corrugated shell plating can be investigated.

- In the study, only a severe storm loading condition is used for the analysis. It is of interest to repeat the design process for normal operation load conditions.

- The production rigs might be built to operate in deeper drafts in the future. It would then be interesting to find the break-even depths where stiffened shell plating becomes favorable compared to corrugated shell plating.

- It may also be interesting to investigate the growth rate increment and cleaning difficulties associated with the corrugated shell plating.

14. References

[1] J.K. Paik and A.K. Thayamballi, Ultimate limit state design of steel-plated structures, John Wiley & Sons (2003).

[2] John R. Saroyan, Coatings and encapsulants - preservers, *Ocean Engineering.* Vol. 1, pp. 435-456. Pergamon Press, Great Britain (1969).

[3] J Kippenes, E Byklum, E Steen, Ultimate Strength of Open Corrugated Panels, *10th International Symposium on Practical Design of Ships and Other Floating Structures*, Houston, Texas, USA, ABS (2007).

[4] J.B. Caldwell, The strength of corrugated plating for ships' bulkheads, *Trans RINA* 97 (1955), pp. 495–522.

[5] J.K. Paik, A.K. Thayamballi and M.S. Chun, Theoretical and experimental study on ultimate strength of corrugated bulkheads, *J Ship Res* 41 (1997), pp. 301–317

[6] SESAM Manuals, 2010.

[7] ABS. Guide for buckling and ultimate strength assessment for offshore structures, 2004.

[8] ABS MODU Rules. (Rules for building and classing mobile offshore drilling units), 2008.

[9] M. K. Rahman, J. B. Caldwell., Rule-based optimization of midship structures, Marine Structures 5 (1992), 467-490.

[10] M.K. Rahman, Optimization of panel forms for improvement in ship structures, Structural Optimization 11, 195-212, Springer-Verlag 1996.

[11] O. Furnes and Ø. Løset, Shell structures in offshore platforms: design and application, pp. 140-152. Det Norske Veritas (1980).

[12] H.H. Sun and J. Spencer, Buckling strength assessment of corrugated panels in offshore structures, Marine Structures, pp. 548-565. Elsevier, USA (2005).

[13] J.K. J.K. Paik and J.K. Seo, Ultimate limit state assessment of ship structures, Pusan National University (2005).

[14] C. Gentilini, K.A. Seffen, S.D. Guest and L. Nobile, On the behavior of corrugated plates in bending, AES – ATEMA 2008.¨

[15] J.K. Paik and A.K. Thayamballi, Some recent developments on the ultimate limit state design technology for ships and offshore structures, Ships and offshore structure, pp. 99-106. Taylor & Francis, London (2010).

[16] A. Romeijn, R. Sarkhosh and H.D. Hoop, Basic parametric study on corrugated web girders with cut outs, Journal of Constructional Steel Research, pp. 395-407, Delft University of Technology (2008).

[17] "Global FE Analysis", Rev.01, GVA-C in-house report, Gothenburg, Sweden, 2007.

[18] "Local FE Analysis Manual: Pontoon and Column", GVA-C in house report, Gothenburg, Sweden, 2007.

[19] G.Y. Grondin, A.E. Elwi and J.J.R. Cheng, Buckling of stiffened steel plates – a parametric study, Journal of Constructional Steel Research, pp. 151-175, University of Alberta, Canada (1998).

[20] H.D. Ji, W.C. Cui and S.K. Zhang, Ultimate strength analysis of corrugated bulkheads considering influence of shear force and adjoining structures, Journal of Constructional Steel Research, p. 525-545, Shanghai Jiao Tong University, (2000).

[21] ABS. Guide for fatigue assessment of offshore structures, 2004.

[22] ABS buckling software (StruProg) manual.

[23] DNV-OS-C102. Offshore standard, Structural design of offshore ships, 2010.

[24] ABS. Fatigue assessment of offshore structures, 2003.

Appendix A: Mesh convergence study
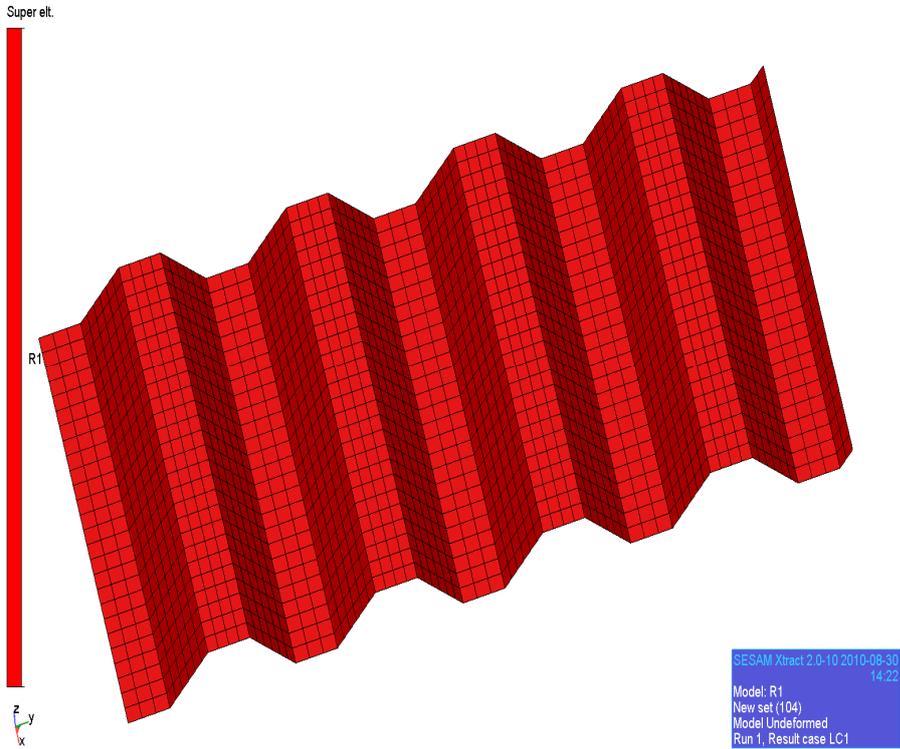
Fig. A1. Portion of the model with 100 mm mesh size.
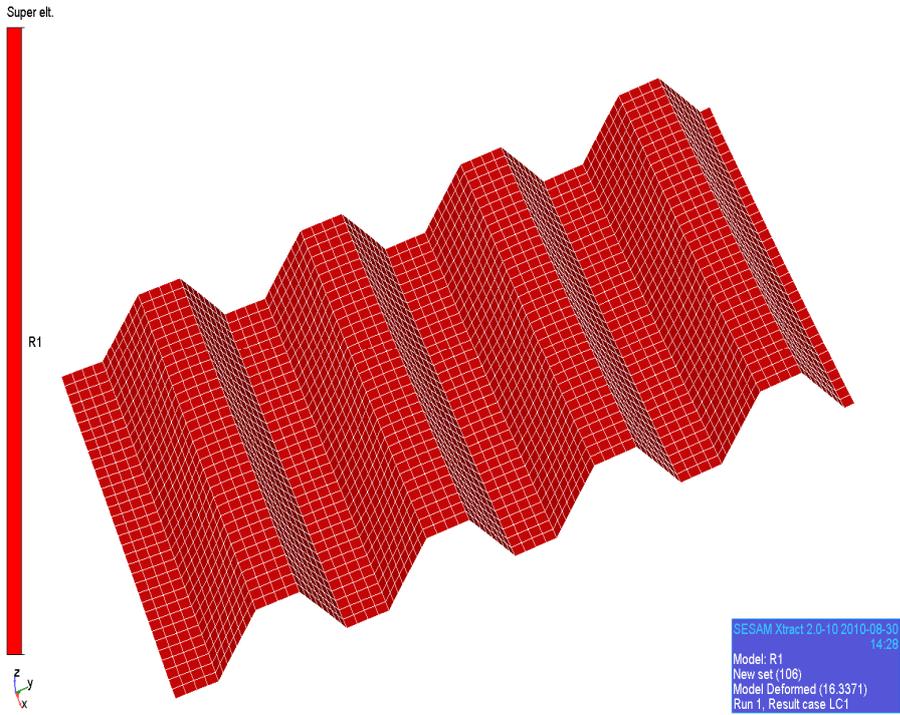
Fig. A2. Portion of the model with 75 mm mesh size.

Appendix B: Simplified fatigue analysis
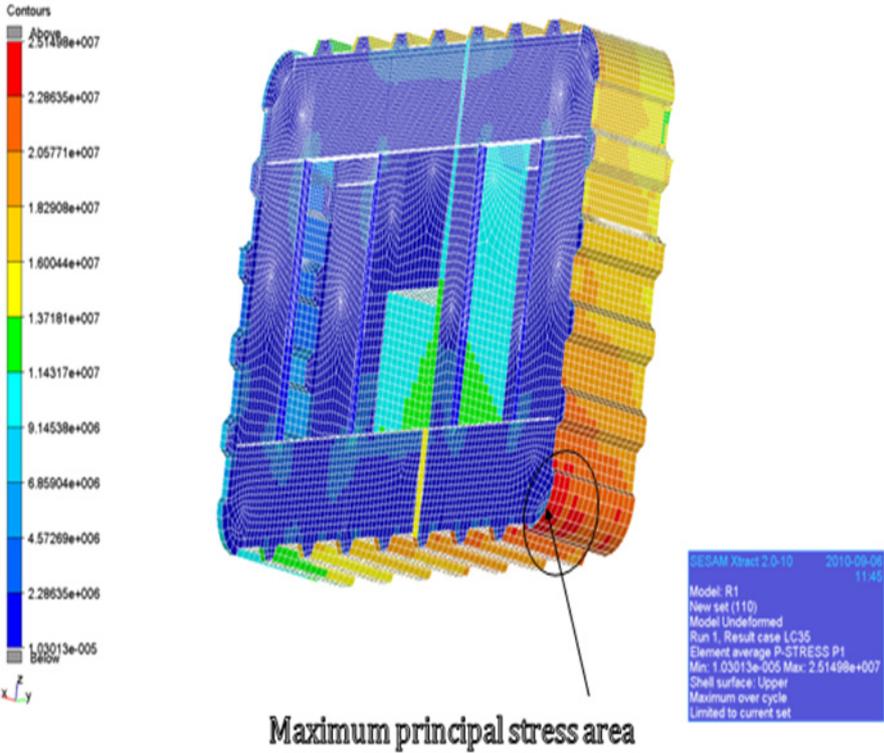
Fig. B1. Simplified fatigue check (measured σ_{xmax} = 25 MPa) on proposal 1.
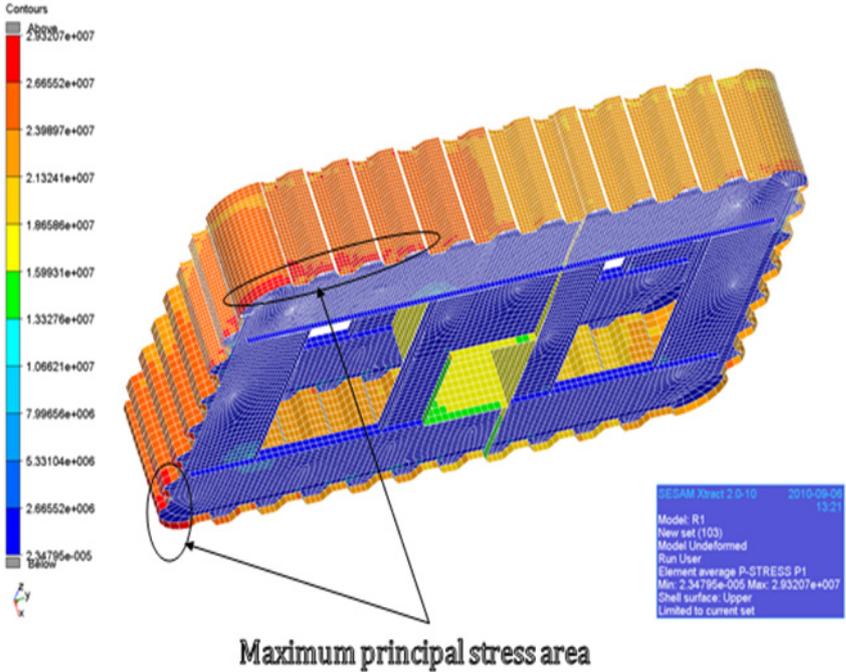
Fig. B2. Simplified fatigue check (measured σ_{xmax} = 29 MPa) on proposal 2.

Appendix C: Mesh pattern
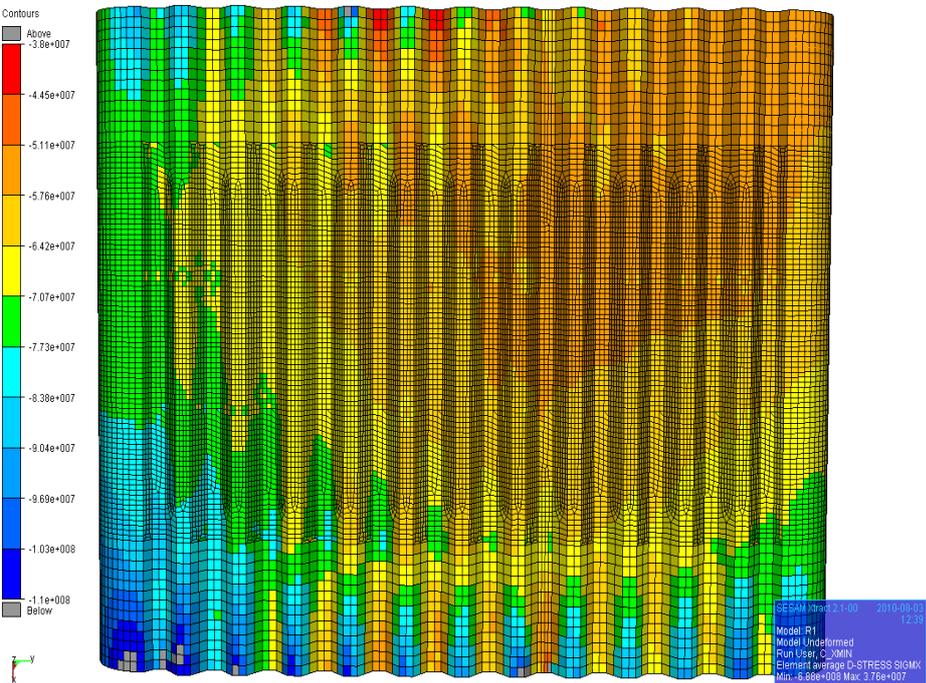
Fig. C1. Five sections with a mesh combination of 200 mm mesh size at the furthest two sections from the mid section and 100 mm mesh size at the three midsections.

Fig. C2. Five sections with 100 mm mesh size all over.

Appendix D: Strength and geometrical features

Table D1. Features of the initial corrugated model with equivalent characteristics of the global pontoon; see Fig. 5.

Component	Level	Magnitude	Unit
Breadth of the panel	B	5120	mm
Length of the panel	L	2560	mm
Width of the upper flange	a	320	mm
Width of the lower flange	b	320	mm
Width of the web plating	c	536	mm
Height of the web plating	d	430	mm
Width of the unit corrugation	s	1280	mm
Plate thickness	t	19	mm
Corrugated panel weight	W_{corr}	2.615	ton
Stiffened panel weight	W_{stiff}	3.599	ton
Weight reduction (%)	-	27.36	%

Table D2. Geometric properties of the final design. Optimum geometric height was achieved.

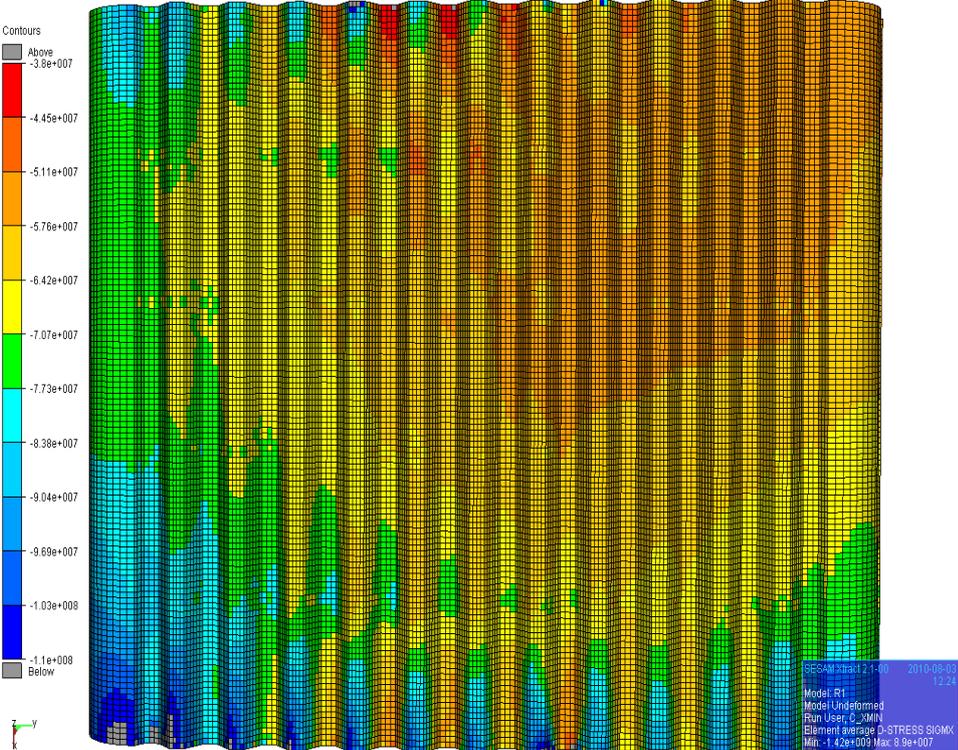| Component	Symbol	Value	Unit
Breadth of the panel	B	5120	mm
Length of the panel	L	2560	mm
Width of the upper flange	a	740	mm
Width of the lower flange	b	920	mm
Width of the web plating	c	310	mm
Height of the web plating	d	260	mm
Width of the unit corrugation	s	1998	mm
Plate thickness	t	19	mm
Corrugation angle	Φ	57.00	degrees
Weight reduction	*	38.01	%

Table D3. Strength characteristics of the final design of proposal 1. The corrugation height was adjusted to sustain local buckling criteria.

Component	Level	Magnitude	Unit
Critical buckling stress in corrugation direction	σ_{Cx}	279	MPa
Critical buckling stress in transverse direction	σ_{Cy}	131	MPa
Critical buckling stress for edge shear	τ_C	183	MPa
Local buckling limit state	*	0.97	Satisfied
Beam-column buckling limit state	*	0.817	Satisfied
Global buckling limit state	*	0.130	Satisfied
US limit state under combined in-plane stresses	*	0.735	Satisfied
US with respect to uniaxial stress in the longitudinal direction	σ_{Ux}	355	MPa
US with respect to uniaxial stress in the y-direction	σ_{Uy}	163	MPa
Ultimate strength with respect to edge shear	τ_U	189	MPa
Equivalent von Mises stress	σ_e	216	MPa
Ultimate strength limit state under lateral pressure	*	0.695	Satisfied

Table D4. Geometrical characteristics of proposal 2 (iteration 1). An equal flange concept was applied with massive thickness reduction.

Component	Level	Magnitude	Unit
Breadth of the panel	B	5120	mm
Length of the panel	L	2560	mm
Width of the upper flange	a	360	mm
Width of the lower flange	b	360	mm
Width of the web plating	c	512.7	mm
Height of the web plating	d	430	mm
Width of the unit corrugation	s	1278.5	mm
Plate thickness	t	12	mm
Corrugation angle	Φ	57	degrees
Weight reduction	*	53.17	%

Table D5. Strength characteristics of proposal 2 (iteration 1). Further thickness reduction to check failure criteria. It sustained at 11mm.

Component	Level	Magnitude	Unit
Critical buckling stress in corrugation direction	σ_{Cx}	288	MPa
Critical buckling stress in transverse direction	σ_{Cy}	133	MPa
Critical buckling stress for edge shear	τ_C	187	MPa
Local buckling limit state	*	0.548	Satisfied
Beam-column buckling limit state	*	0.738	Satisfied
Global buckling limit state	*	0.112	Satisfied
US limit state under combined in-plane stresses	*	0.546	Satisfied
US with respect to uniaxial stress in the long. dir.	σ_{Ux}	287	MPa
US with respect to uniaxial stress in the y-direction	σ_{Uy}	107	MPa
Ultimate strength with respect to edge shear	τ_U	190	MPa
Equivalent von Mises stress	σ_e	169	MPa
Ultimate strength limit state under lateral pressure	*	0.530	Satisfied

Table D6. Geometrical characteristics of proposal 2 (iteration 3). The flange width was increased and the thickness kept constant.

Component	Level	Magnitude	Unit
Breadth of the panel	B	5120	mm
Length of the panel	L	2560	mm
Width of the upper flange	a	450	mm
Width of the lower flange	b	450	mm
Width of the web plating	c	441.2	mm
Height of the web plating	d	370	mm
Width of the unit corrugation	s	1380.6	mm
Plate thickness	t	11	mm
Corrugation angle	Φ	57	degrees
Weight reduction	*	59.4	%

Appendix E: Stiffener features
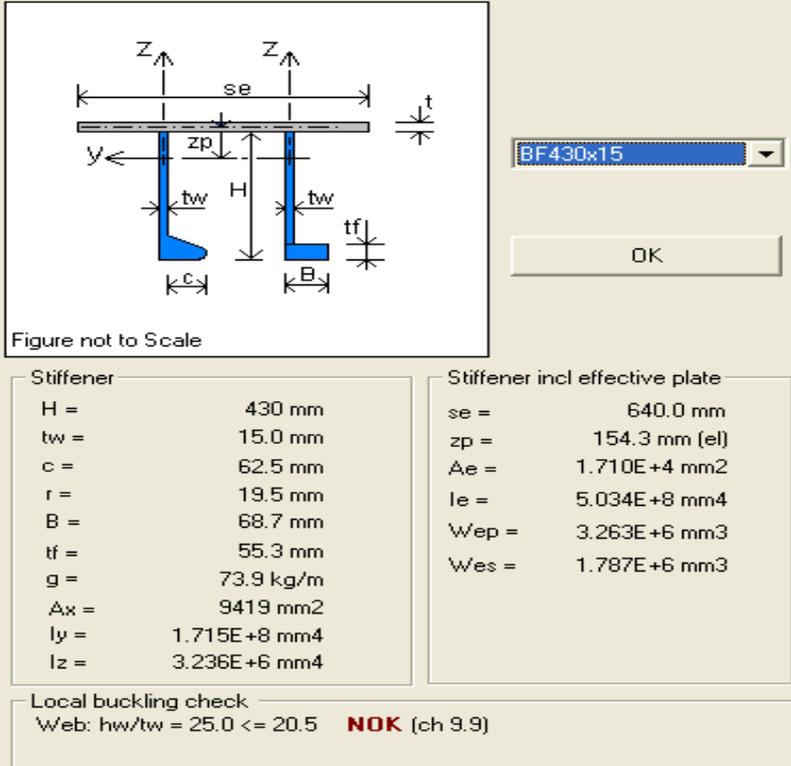
Fig. E1. Initial stiffener scantlings. This was applied to the reference model.
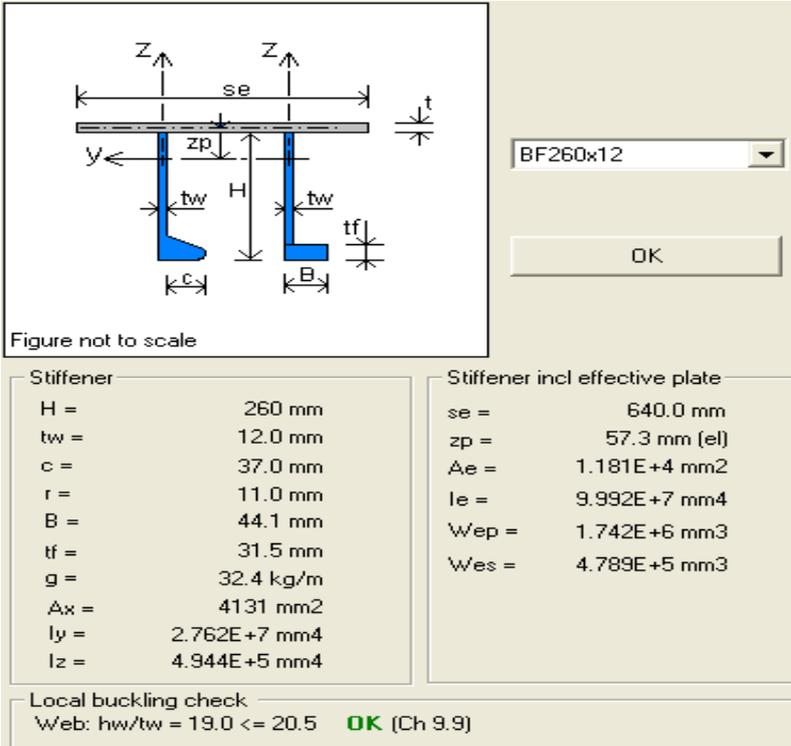
Fig. E2. Final stiffener scantlings. After an FEA and a numerical iterative process, this stiffener scantling was achieved, which narrowly passed the buckling criteria.

Appendix F: Parametric study curves
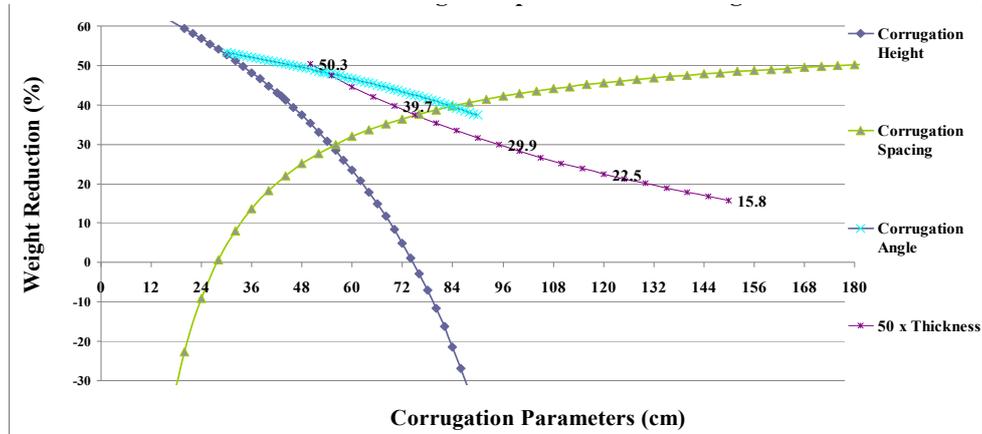
Fig. F1. Influence of corrugation parameters on weight. Weight reduction of the corrugated panel compared to the stiffened panel when different parameters are varied.
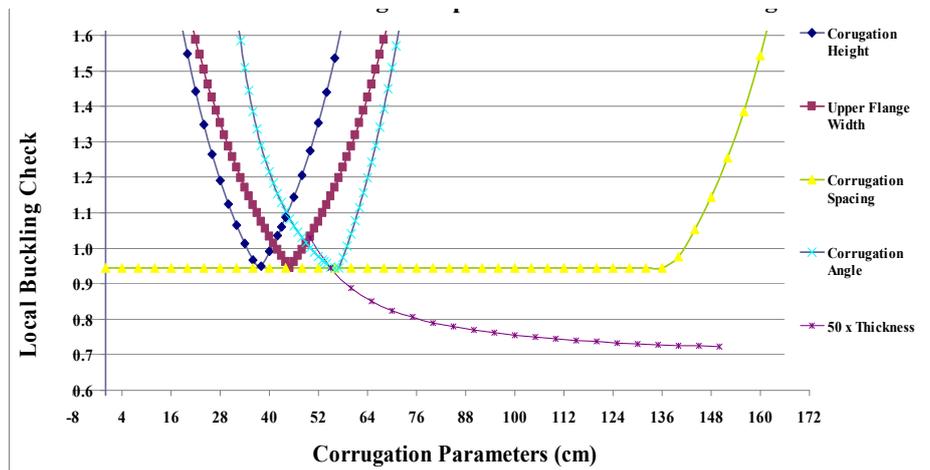
Fig. F2. Influence of corrugation parameters on local buckling limit state. This buckling study looks for the points of minima in a variation of corrugation parameters.
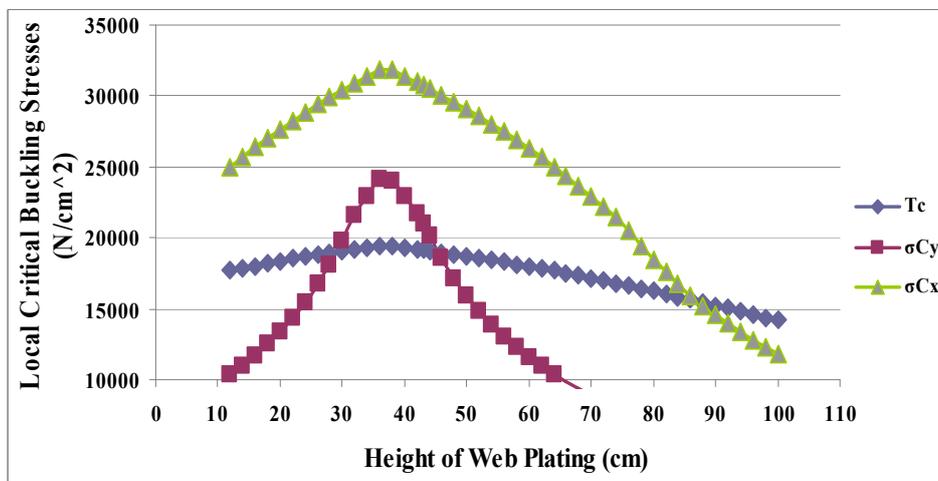
Fig. F3. Influence of height of web plating on local critical buckling stress. This study looks for the maximum limit points of the responses both in bi-axial and shear stresses.

59
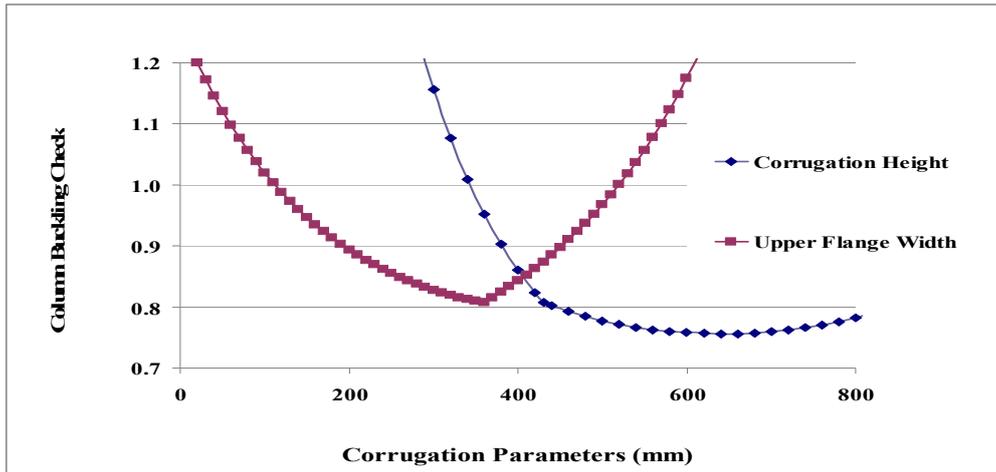
Fig. F4. The influence of corrugation parameters to beam-column buckling capacity. This figure was employed to decide on the next iteration during the design process of the second proposal.
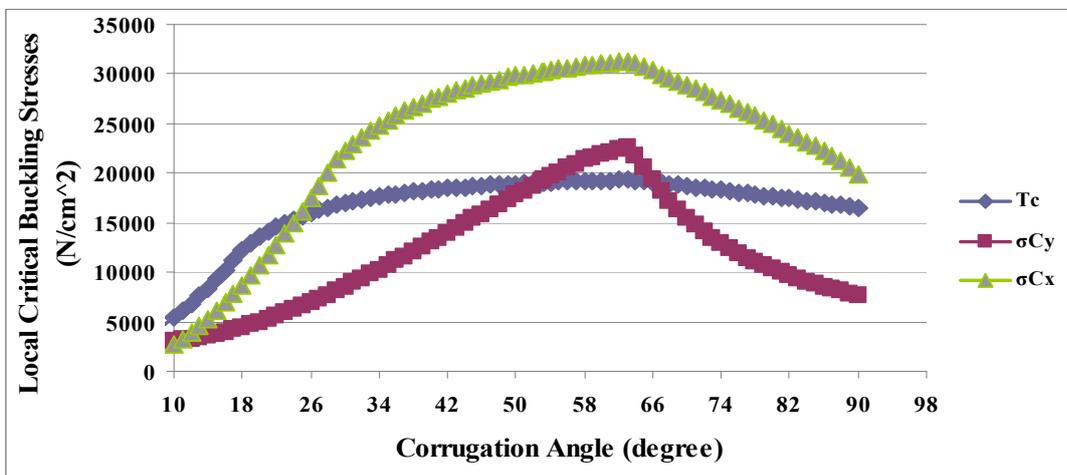
Fig. F5. Influence of corrugation angle on local critical buckling stresses. This study narrows down the search for a suitable corrugation angle; 57 degrees was concluded to be the most effective corrugation angle and was maintained throughout the study.
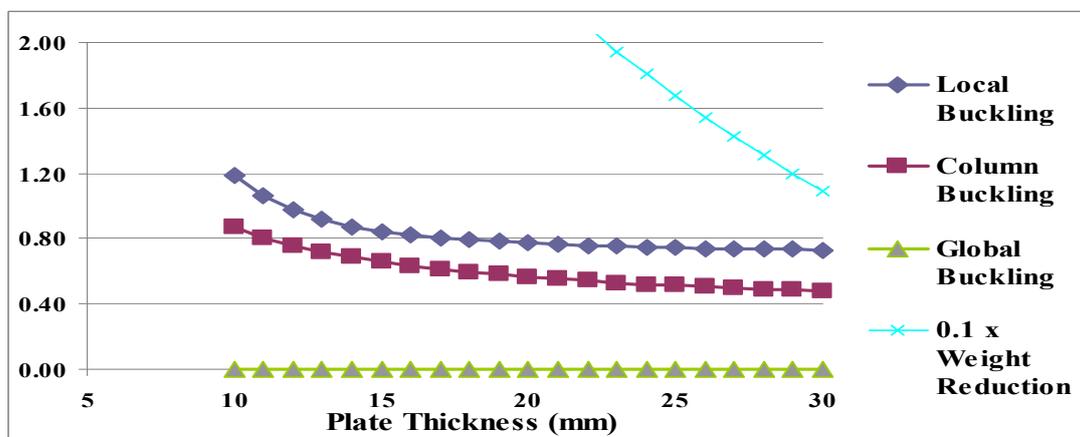
Fig. F6. Influence of thickness to different buckling failure modes and panel weight. This figure was employed during the second design proposal explained in Chapter 7.

Appendix G: ABS StruProg software output

A B S P S	Project: Optimization of pontoon structure with stiffe	Page:
	ned shell plating	1/1
Version 1.3 Plate/Stiff. check based on ABS Offshore Structures Copyright (C) 2009 StruProg AB	Identification: Ex1	Date: 11/12/2010
		Time: 18:18
File: c:\progra~1\strupr~1\abspsd~1.3\dummy.abso		

Safety format/Material:

Loading Condition   B
Plate/Stiffener: H 36/H 36
Yield stress   Fyp/Fys =   355/355   MPa
Tensile stress   Fup/Fus =   490/490   MPa
Youngs modulus   E   =   2.06E+5   MPa

Geometry:

Stiffener span	L	=	2560	mm
Plate thickness	t	=	13.0	mm
Stiffener spacing	s1	=	640	mm
	s2	=	640	mm
Unit length	UL	=	65	m

Watertight bulkhead / Stiffener: ends attached
                                  c   =   0.56

Figure:

Stresses:

SigxA	=	-96.0	MPa
SigxB	=	-96.0	MPa
SigyA	=	-50.0	MPa
SigyC	=	-50.0	MPa
Tau	=	51.0	MPa
p	=	0.316	MPa (On stiff side)

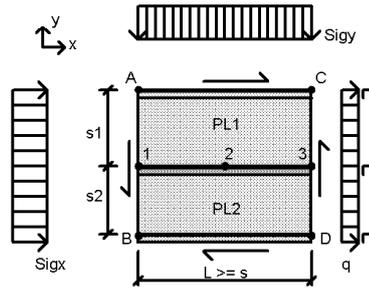*Stiffener:* BF 260x12.0

Stiffener property:				Incl. eff. plate:			
H	=	260	mm	se	=	640.0	mm
tw	=	12.0	mm	zp	=	54.6	mm
c	=	37.0	mm	Ae	=	1.245E+4	mm2
r	=	11.0	mm	Ie	=	1.024E+8	mm4
B	=	44.1	mm	Wep	=	1.877E+6	mm3
tf	=	31.5	mm	Wes	=	4.831E+5	mm3
A	=	4131	mm2	Web: hw/tw = 19.0 <= 20.5 **OK** (Ch 9.9)			
g	=	32.4	kg/m				
ez	=	158.0	mm				
Iy	=	2.762E+7	mm4				
Iz	=	4.944E+5	mm4				

(Rule/Buckling: ABS-Buckling and Ultimate Strength Assessment for Offshore Structures)

PLATE BUCKLING CONTROL:

PL1: Buckling - UF =SQR((-96.0/256.6)^2 + (-50.0/95.4)^2 + (51.0/181.5)^2) =   **0.70** < 0.80 (Sec 3, Ch 3.1)
PL1: Ultimate - UF = SQR((-96.0/262.4)^2 --0.02*(-96.0*-50.0/(262.4*106.5) + (-50.0/106.5)^2 + (51.0/185.9))^2) =   **0.66** < 0.80 (Sec 3, Ch 3.3)
PL1/PL2: Lateral - UF = p/pu = 0.316/0.585 =   **0.54** < 0.80 (Sec 3, Ch 3.5)
PL2: Buckling - UF =SQR((-96.0/256.6)^2 + (-50.0/95.4)^2 + (51.0/181.5)^2) =   **0.70** < 0.80 (Sec 3, Ch 3.1)
PL2: Ultimate - UF = SQR((-96.0/262.4)^2 --0.02*(-96.0*-50.0/(262.4*106.5) + (-50.0/106.5)^2 + (51.0/185.9))^2) =   **0.66** < 0.80 (Sec 3, Ch 3.3)
PL1/PL2: Lateral - UF = p/pu = 0.316/0.585 =   **0.54** < 0.80 (Sec 3, Ch 3.5)

STIFFENER BUCKLING CONTROL:

Buckling, se = 640.0 mm   Bending, sw = 480.0 mm
UFbu= 96.0/(343.1*(12451/12451)) + 0.75*233.8/(355.0*[1-96.0/(0.80*2551.4)]) =   **0.80** < 0.80 (Sec 3, Ch 5.1)
UFbt= Siga/SigCT = 96.0/297.9 =   **0.32** < 0.80 (Sec 3, Ch 5.3)

STIFFENER DEFORMATION CHECK: (Based on effective plate width as sw)

Deformation y = p*(s1+s2)/2*l^4/(384*E*lyeff) = 0.32*(640+640)/2*2560^4/(384*E*94.9E+6) = **1.2 mm** ==> l/2213

(Rule/Scantling, Yield: ABS, Mobile Offshore Drilling Units, Part 3 Hull Construction and equipment)

PLATE YIELD CONTROL: Control in points A-D, Factor of Safety F.S. = 1.11
Point: A: UF = Sigeq/Fy = 121.3/355.0 =   **0.34** < 0.90 (3-2-1/3.11)

STIFFENER YIELD CHECK: (check at points 1-3, plate(p) and stiffener(s)). Effective width sw = 640.0 mm
Point 1p: UF = Sigeq/Fy = 162.9/355.0 =   **0.46** < 0.90 (3-2-1/3.11)
Point 2s: UF = Sigeq/Fy = 210.3/355.0 =   **0.59** < 0.90 (3-2-1/3.11)

Fig. G1. Buckling and yield check of the final stiffened pontoon design.This is a standard STRUPROG output sheet and the column buckling and deformation was checked against a limit of 0.8. However, for yield check this limit becomes 0.9. This program was used for modification of the initial reference model with the use of response stresses obtained from the FEA.

Appendix H: Buckling strength assessment

Table H1. Buckling strength assessment of the flange and web plate panels at the local level for the initial model. The highest stress at 70 percent of the area is considered. At this level, load carrying capacity does not exhaust even by fifty percent.

Component	Level	Magnitude	Unit
Modulus of elasticity	E	2.06E+05	MPa
Proportional linear elastic limit of the structure	P_r	0.6	-
Specified minimum yield point of plate	σ_o	355	MPa
Poisson's ratio (for steel according to ABS)	N	0.3	-
Length of short plate edge	M	536	mm
Aspect ratio for local buckling	α_L	4.78	-
Ratio of edge stresses (x)	K	0.795	-
Ratio of edge stresses (y)	K	0.330	-
Factor 1 for x-direction (for local plate of panel)	C_1	1	-
Factor 2 for y-direction (for local plate of panel)	C_2	1	-
Buckling coefficient for the x-direction	k_s	4.43	-
Buckling coefficient for the y-direction	k_{s1}	1.582	-
Buckling coefficient for y-direction (for $\kappa > 1/3$)	k_{s2}	-	-
Boundary dependent constant for edge shear	k_s	5.515	-
Elastic buckling stress (x)	σ_{Ex}	1038	MPa
Elastic buckling stress (y)	σ_{Ey}	370	MPa
Elastic shear buckling stress	τ_E	1291	MPa
Critical buckling stress (x)	σ_{Cx}	326	MPa
Critical buckling stress (y)	σ_{Cy}	273	MPa
Critical buckling stress for edge shear	τ_C	197	MPa
Adjustment factor	Ψ	0.87	-
Max. allowable strength utilization factor	H	0.696	-
Local buckling limit state	0.479	satisfied	-

Table H2. Buckling strength assessment of unit corrugation. A unit corrugation is chosen close to the left bilge of the section in Fig. 13. The average FEA response of the total corrugation unit is considered as a response input to numerical validation.

Component	Level	Magnitude	Unit
Radius of gyration of area	r	164.10	mm
Section modulus	SM	0.004076	m^3
Coefficient	k_c	47.89	-
Lateral pressure at the first end of the corrugation	q_u	0.3016	MPa
Lateral pressure at the second end of the corrugation	q_l	0.3016	MPa
Max. bending moment induced by lateral pressure	M_b	210856	Nm
Bending moment factor for a simple support panel	C_m	1.5	-
Elastic buckling stress of unit corrugation	$\sigma_{E(B)}$	3185	MPa
Critical bending buckling stress	σ_{cb}	345.50	MPa
Elastic buckling stress	$\sigma_{E(C)}$	8364	MPa
Critical buckling stress	σ_{Ca}	351.38	MPa
Maximum bending stress along the length due to lateral pressure	σ_b	51.73	MPa
Adjustment factor	Ψ	0.87	-
Max. allowable strength utilization factor (severe storm)	η	0.696	-
Beam-column buckling limit state	0.665	satisfied	-

Appendix I: Ultimate strength assessment

Table I1. Ultimate strength check under combined loading of in-plane stresses.

Component	Level	Magnitude	Unit
Modulus of elasticity	E	2.06E+05	MPa
Proportional linear elastic limit of the structure	P_r	0.6	-
Poisson's ratio (for steel according to ABS)	ν	0.3	-
Length of the panel	L	2560	mm
Length of short plate edge	m	536	mm
Plate thickness	t	19	mm
Specified minimum yield point of plate	σ_o	355	MPa
Slenderness ratio	β	1.171	-
Coefficient	C_x	0.979	-
Coefficient	C_y	0.441	TRUE
Coefficient to reflect interaction between longitudinal	Ψ	0.414	-
Critical buckling stress (x-direction)	σ_{Cx}	325.9	MPa
Critical buckling stress (y-direction)	σ_{Cy}	273.33	MPa
Critical buckling stress (shear)	τ_C	197.15	MPa
US with respect to uniaxial stress in the x-direction	σ_{Ux}	347 MPa	TRUE
US with respect to uniaxial stress in the y-direction	σ_{Uy}	157 MPa	FALSE
Ultimate strength with respect to edge shear	τ_U	198 MPa	TRUE
Adjustment factor (for axial tension and bending)	Ψ	0.87	-
Max. allowable strength utilization factor (severe storm)	η	0.696	-
Ultimate strength capacity	0.44	satisfied	-

Table I2. Ultimate strength check under lateral pressure within plane stresses. The plate panel is preferred to be buckled before it fails. In this case, up to a certain depth it does not buckle under lateral pressure of water.

Component	Level	Magnitude	Unit
Lateral pressure at the first end of the corrugation	q_u	0.3016	MPa
Aspect ratio	α_L	4.78	-
Specified minimum yield point of plate	σ_o	355	MPa
Plate thickness	t	19	mm
Length of short plate edge	m	536	mm
Equivalent von Mises stress	σ_e	154	MPa
Adjustment factor (for axial tension and bending)	Ψ	0.87	-
Max. allowable strength utilization factor (severe storm)	η	0.696	-
Ultimate strength capacity	0.225	satisfied	-

Appendix J: Cost model

Cost formulations
(1) Material cost for hull plates: $C_1 = AT_{ps} \times P_p \times 7.85 \times 1$
(2) Material cost for longitudinal: $C_2 = (2AT_{ss} + AT_{sd} + AT_{sb}) \times P_t \times 7.85 \times 1$
(3) Material cost for transverse web frame: $C_3 = A_{wf} \times P_p \times 7.85$
(4) Material cost for longitudinal: $C_4 = (2N_{lgs} + 2N_{lg}) \times P_{wc} \times 1$
(5) Material cost for transverse web frame, bulkhead and tunnel: $C_5 = P_{wc} \times W_{lf} \times 3$
(6) Welding cost for shell plating: $C6 = P_{wc} \times W_{lp} \times 1$
(7) Painting cost for shell plating: $C7 = C_{s5} \times A_{tps} \times P_{mp}$
(8) Painting cost for web frame, bulkhead and tunnel plating: $C_8 = C_{s6} \times A_{oth} \times P_{mp} \times 4$
(9) Painting cost for longitudinal: $C_9 = (2N_{lgs} + 2N_{lg}) \times P_{wc} \times 1$

TOTAL COST: $\sum C_N$

Unit cost formulation
1. Shell plate (Euro/ton): $P_p = C_{a1} \times P_a$
2. Standard sections for longitudinal (Euro/ton): $P_t = C_{a2} \times P_a$
3. Standard sections for transverse webs (Euro/ton): $P_t = C_{a3} \times P_a$
4. Cost of welding of longitudinal to plates (Euro/m): $W_t = C_{s1} \times P_s$
5. Cost of welding of transverse web plates (Euro/m): $W_t = C_{s2} \times P_s$
8. Cost of electricity and electrodes for welding (Euro/m): $E_c = C_{s4} \times P_s$

Table J1. Cross sectional area definition.

Symbol	Description
AT_{ps}	Total cross-sectional area of plates (m^2)
AT_{ss}	Total cross-sectional area of side longitudinal (m^2)
AT_{sd}	Total cross-sectional area of deck longitudinals (m^2)
A_{oth}	Total area of web frame, bulkhead and tunnel (m^2)
AT_{sb}	Total cross-sectional area of bottom longitudinals (m^2)
A_{wf}	Cross-sectional area of web frame (m^2)
A_{wf}	Cross-sectional area of tunnel + longitudinal bulkhead (m^2)
N_{lg}	Number of longitudinals in deck or bottom
Nl_{gs}	Number of longitudinals in sides
W_{lf}	Web frame, bulkhead and tunnel welding length, m
W_{lp}	Shell plate welding length, m

Table J2. Cost factors considered for present study.

Component	Factor	Magnitude	Unit
Steel	C_{a1}	1	
Longitudinal	C_{a2}	1.25	
Web frame	C_{a3}	1	
Longitudinal + plate welding rate	C_{s1}	0.1	h/m
Web frame + plate welding rate	C_{s2}	0.1	h/m
Welding rate	C_{s4}	0.1	h/m
Paint factor (exposed to water)	C_{s5}	0.8	litre/m^2
Paint factor (inside)	C_{s6}	0.15	litre/m^2